Summer 8-31-2000

Nanofiltration-based diafiltration process for solvent exchange in pharmaceutical manufacturing

Jignesh P. Sheth
New Jersey Institute of Technology

ABSTRACT

NANOFILTRATION-BASED DIAFILTRATION PROCESS FOR SOLVENT EXCHANGE IN PHARMACEUTICAL MANUFACTURING

by
Jignesh P. Sheth

Commercially available solvent stable polymeric nanofiltration membranes were used to study the nanofiltration and diafiltration operations in the context of the pharmaceutical industry. Experimental results are presented for a two-step operation involving the pre-concentration of a feed solution via nanofiltration followed by the replacement of the first stage solvent with a second solvent via diafiltration in two stages. Membranes MPF-50 and MPF-60, having molecular weight cut-offs of 700 and 400 respectively, were used in the present study. A solution of erythromycin (MW 734) in ethyl acetate was pre-concentrated via nanofiltration followed by replacement of ethyl acetate with methanol via batch diafiltration. The experiments were carried out at 440 psig (3033.8 kPa) and room temperature. Membrane compaction, during the initial period of each operation, affected the solute rejection and permeate flux. High erythromycin rejection (96 % +) was achieved with the MPF-60 membrane. During the diafiltration operations the membranes exhibited no selectivity for the solvent mixture, irrespective of the feed concentration. Ethyl acetate concentration was reduced to less than 4 % over two batch diafiltration runs.

NANOFILTRATION-BASED DIAFILTRATION PROCESS FOR SOLVENT EXCHANGE IN PHARMACEUTICAL MANUFACTURING

by
Jignesh P. Sheth

A Thesis
Submitted to the Faculty of
New Jersey Institute of Technology
in Partial Fulfillment of the Requirements for the Degree of
Master of Science in Chemical Engineering

Department of Chemical Enginering,
Chemistry and Environmental Science

August 2000

APPROVAL PAGE

NANOFILTRATION-BASED DIAFILTRATION PROCESS FOR SOLVENT EXCHANGE IN PHARMACEUTICAL MANUFACTURING

Jignesh P. Sheth

Dr. Kamalesh K. Sirkar, Advisor — Date
Distinguished Professor of Chemical Engineering,
Sponsored Chair, Membrane Separations and Biotechnology, NJIT

Dr. Basil C. Baltzis, Co-Advisor — Date
Professor of Chemical Engineering, NJIT

Dr. Sanjay V. Malhotra, Committee Member — Date
Assistant Professor of Chemistry NJIT

BIOGRAPHICAL SKETCH

Author: Jignesh P. Sheth

Degree: Master of Science in Chemical Engineering

Date: May 2000

Undergraduate and Graduate Education:

- Master of Science in Chemical Engineering,
  New Jersey Institute of Technology, Newark, NJ, 2000

- Bachelor of Engineering in Chemical Engineering
  Shivaji University, Kolhapur, India. 1996

Major: Chemical Engineering

Presentations and Publications:

Sheth, J. P., Y. J. Qin, B. C. Baltzis, and K. K. Sirkar, "Nanofiltration-Based Diafiltration Process for Solvent Exchange in Pharmaceutical Manufacturing," *North American Membrane Society Annual Meeting*, Boulder, CO, May, 2000.

Qin, Y. J., J. P. Sheth, and K. K. Sirkar, "Removal and Recovery of Apolar and Polar VOCs from Water by SLM-Based Pervaporation," *North American Membrane Society Annual Meeting*, Boulder, CO, May, 2000.

Qin, Y. J., J. P. Sheth and K. K. Sirkar, "Supported Liquid Membrane Based Pervaporation," *AIChE Spring Meeting*, Atlanta, GA, March, 2000.

Qin, Y. J., G. Obuskovic, J. P. Sheth, S. Majumdar and K. K. Sirkar, "Supported Liquid Membranes in Pollution Control for Liquid and Gaseous Streams," *AIChE Annual Meeting*, Dallas, TX, November, 1999.

This thesis is dedicated to my parents and my sister,
who have been constants when everything else was variable.

ACKNOWLEDGEMENT

I am grateful to my advisors, Dr. Kamalesh K. Sirkar and Dr. Basil C. Baltzis for their guidance and encouragement throughout this research. I thank Dr. Sanjay V. Malhotra for serving as a member on my thesis committee.

I thank the Emissions Reduction Research Center, the Membrane Separations and Biotechnology Program and the Center for Membrane Technologies for providing financial support for this project

Working with Dr. Yingjie Qin has been a valuable learning experience and I sincerely thank him. Many intractable problems were simplified by the resourcefulness of the members of the Membrane Separations and Biotechnology Group. They have made my stay at the New Jersey Institute of Technology memorable and I sincerely thank them.

TABLE OF CONTENTS

TABLE OF CONTENTS
(Continued)

Chapter **Page**

TABLE OF CONTENTS
(Continued)

Chapter **Page**

LIST OF TABLES

Table **Page**

LIST OF FIGURES

LIST OF SYMBOLS

A_m : total membrane area, m^2

c_i : concentration of species *i* in the membrane, mol m^{-3}

C_i : concentration of species *i*, mol m^{-3}

d_p : pore diameter of membrane layer *i* (*i* = 1,2), m

D : bulk diffusivity, m^2 s^{-1}

D_e : effective diffusivity, m^2 s^{-1}

f : friction coefficient

f_1 : membrane parameter, defined in equation (2.10), dimensionless

f_2 : membrane parameter, defined in equation (2.11), dimensionless

J_i : molar flux of species *i*, mol m^{-2} s^{-1}

J_s : solvent flux through the membrane, L m^{-2} s^{-1}

J_{sm} : mixed solvent flux, L m^{-2} s^{-1}

k_M^i : constant describing pore characteristics of membrane layer, *i*, (*i*=1,2), m

K_{ic} : hindrance factor for convection, dimensionless

K_{id} : hindrance factor for diffusion, dimensionless

L_p : membrane permeability, L m^{-2} s^{-1} / psi m^{-1}

L_p' : apparent permeability of membrane, defined in equation (2.3)

P : pressure, psig

Pe_m : Peclet number, defined in equation (2.18), dimensionless

r_p : hydrodynamic pore radius, nm

LIST OF SYMBOLS
(Continued)

R : Universal gas constant

R_S^0 : surface resistance, Pa s m^{-1}

R_μ^i : viscous resistance of the membrane layer, i, (i=1,2), Pa s m^{-1}

T : absolute temperature, K

t : operation time, s

V : volume of feed solution, L

$\bar{V}$: volume fraction, dimensionless

X : effective membrane charge density, mol m^{-3}

Greek Letters

γ_M : critical membrane surface tension, mN m^{-1}

γ_S : solvent surface tension, mN m^{-1}

γ_i : activity coefficient of the ion in the interface, dimensionless

Δ : difference between the feed and permeate phases, dimensionless

δ : membrane thickness, m

ε : membrane porosity, dimensionless

η : viscosity of solution inside the pore, g m^{-1} s^{-1}

ϕ : partition coefficient, defined in equation (2.17)

μ : solvent viscosity, Pa s

Π : osmotic pressure, psig

τ : membrane tortuosity, dimensionless

φ : solvent parameter, defined in equation (2.12)

ψ : electrical potential in the axial direction, V

$\Delta\psi_D$: Donnan potential, V

Subscripts

c : convection

d : diffusion

i : species *i*

m : membrane

0 : in bulk solution

p : permeate

r : retentate

s : solvent

so : original solvent

sr : replacement solvent

l : large molecular weight solute

CHAPTER 1

INTRODUCTION

1.1 General Background

Manufacturing activities within the chemical process industry (CPI) can be classified into chemical processes, which involve the synthesis of various chemicals and unit operations, which involve the isolation of products from various byproducts. With the increasing sophistication of end-use applications, greater demands are being put on the field of separations to isolate products more completely and at lower costs. This is especially true in the pharmaceutical industry, which generally produces high value products. In such applications, economics become very sensitive to the ability of the separation processes to minimize waste and isolate products of interest completely.

Most pharmaceutical products (intermediate or final) are thermally sensitive and hence require great care during their separation. Vacuum distillation, solvent extraction, etc. have been traditionally employed to effect separation of these products from their solvent media. However, the heterogeneous nature of most pharmaceutical reactions, that involve intermediates and active components in the molecular weight range of 300 to 1000 daltons (Paul et al, 1990), can be advantageously exploited by non-conventional separation processes involving selective membranes to effect separation.

Membrane separation technology has come a long way since the invention of the first integrally skinned hyperfiltration (reverse osmosis) membrane by Loeb and Sourirajan in 1960. Recent developments in this field has enabled it to overcome the commercialization barrier, so much so that today the worldwide annual installed gas handling capacity of membrane systems has reached 4 billion m^3 and is set to grow at the

rate of 8 % per annum (Puri, 1999). The total sale of membrane materials is expected to reach more than $1.5 billion by 2002, with liquid-solid separation applications in the field of wastewater treatment and food and beverage industry accounting for more than 60 % of the total consumption (Rogers, 1998). Liquid-solid membrane separation processes are generally pressure driven, carried out at ambient temperature. Combined with their modular nature (which facilitates capacity modification), competitive economics, ambient temperature separation, and elimination of extraneous hazardous chemicals to effect separation have made them particularly attractive to an industry that produces thermally labile, high value products.

1.2 Liquid-Solid Membrane Separation Processes

Reverse osmosis (RO), ultrafiltration (UF), microfiltration (MF) and more recently, nanofiltration (NF), are pressure driven separation processes that employ permselective membranes to separate dissolved inorganic/organic species. Distinction between these processes is primarily made on the basis of the magnitude of the applied transmembrane pressure and the size of the particles retained. Figure 1.1 illustrates the pore sizes of RO, UF, NF, and MF membranes along with characteristic particle sizes retained. RO membranes are essentially nonporous.

RO and UF are well established membrane-based pressure driven operations primarily used in the separation of aqueous solutions. NF however, is a relatively recent development in this field. NF membranes are a new class of membranes with properties in between those of RO and UF (Bowen et al., 1998). Separation mechanisms differ in each of these processes. A classical model to describe solute rejection in RO is based on

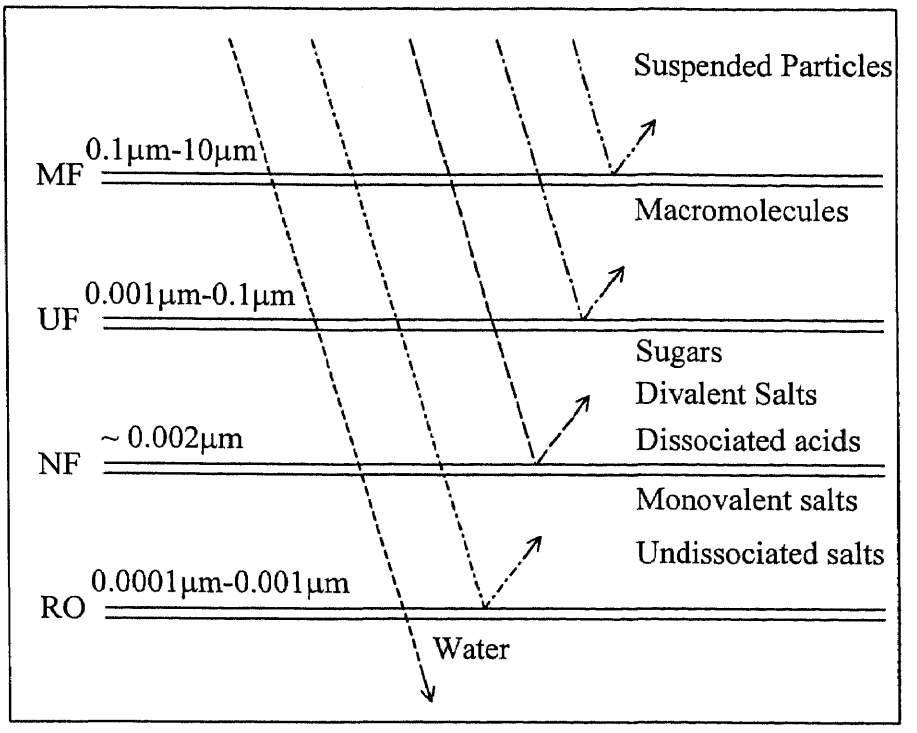

Figure 1.1 Filtration Range and Membrane Pore Size as Applied to Aqueous Systems (adapted from Raman et al., 1994 and Porter, 1988)

the Solution–Diffusion model which assumes that both solute and solvent dissolve in the microporous membrane and then each diffuses across it at a different rate, independent from each other, thereby effecting separation (Lonsdale, 1965). Rejection of solutes in UF, on the other hand, is based on a sieving mechanism in which the solvent flows through the pores, convectively carrying along with it solute molecules smaller than the pore size of the membrane (Blatt et al., 1970). Segregation properties of NF membranes, however, depend on several parameters like streic forces (for neutral species) or electrostatic forces and charge density of the ion (for charged species), determined by the treatment employed during membrane fabrication and end-use application requirements.

1.3 Nanofiltration

1.3.1 Historical Background

The term "nanofiltration", based on an analogous definition of microfiltration where micron (μm) is the unit of measure for characterizing the nominal minimal particle size retained by the membrane, has been coined in 1986; in the case of nanofiltration, molecules on the order of a nanometer are retained (Eriksson, 1986). Generally the nominal molecular weight cutoff ranges from 100 to 200 daltons (Raman et al., 1994). Sometimes referred to as membrane softening, NF has been traditionally used to remove divalent ions of calcium and magnesium from drinking water. The first commercial demineralization/desalination membrane softening system (M/B 5575) was made available by a Florida based equipment manufacturer in the mid-1970s (Culler et al.,1976). The system offered as an alternative to conventional lime softening to treat hard and mildly brackish shallow groundwater, utilized a modified RO membrane and operated at 200 psig (as opposed to 400psig in RO). The cellulose diacetate membrane had an approximate total dissolved solids (TDS) rejection in the range of 55 % for monovalent ions such as sodium and chloride to 75 % for divalent ions such as calcium, magnesium and sulfates. The membrane was also able to reject bacteria and viruses. But the introduction of low pressure (200-300 psig) cellulose triacetate hollow fiber and thin-film composite polyamide spiral-wound RO membranes in the 1980s having TDS rejection in excess of 95 %, made this process economically unattractive. It was not until the introduction of thin-film composite cross-linked polyamide NF membranes (capable of operation in the 70-150 psig range) that NF became an economically viable unit operation.

1.3.2 Separation Mechanism

The separation of solutes (inorganic/organic) via NF depends upon several parameters including streic (sieving) and hydrodynamic forces (Rosa et al., 1994), electrostatic and dielectric forces, the hydration state of the molecules (Macoun et al., 1991), Donnan effect (Tsuru et al., 1994) or the combination of hydrodynamic and electrostatic forces (Pontalier et al., 1996). Application of NF has traditionally been confined to aqueous systems and several models describing the separation mechanism exist. Two categories of models exist to describe retention of charged and uncharged molecules, respectively.

Models that describe the retention of charged molecules can be further sub-divided into space-charge models and fixed-charge models. The space-charge model takes into account the distribution of potential and ions in the radial and axial direction within microcapillaries. Nernst-Planck equation describes the transport and the Stokes equation is used to calculate the volumetric flow (Morrison et al., 1965). Parameters required for the model cannot be determined by separate measurements of membrane and solution properties. This is a major drawback (Hagmeyer et al., 1999). The more recent Teorell, Meyer and Sievers–extended Nernst Planck model (TMS-NP) is a fixed charged model. It is a simplification of the space-charge model in that it neglects radial distributions in a pore. This model is in good agreement with the space-charge model, if the pore radius is much lower than the Debye length (Wang et al., 1995). A uniform surface charge distribution and electroneutrality of ions and volume charge in the pore are assumed in this model and the transport through the pore is calculated using the Nernst-Planck equation extended for convection. This model has been successfully applied to predict the rejection of binary and ternary ion mixtures.

Models that describe the retention of uncharged molecules are based on the pore size of the membrane and the solute molecules. The streic hindrance pore model (SHP) assumes that all membrane pores have the same size. Steric hindrance and interactions with the pores prevent the passage of molecules, having the same size (or larger) as the pore, through the membrane completely. Molecules smaller than the membrane pore size are retained partially (Wang et al., 1995; Wang et al., 1997). The model developed by Zeman and Wales (1981)describes the rejection of a sphere through a cylindrical capillary of uniform diameter and assumes a parabolic velocity profile within a pore. The log-normal model on the other hand assumes a log-normal distribution of the pore size. Streic hindrance within the pores or hydrodynamic drag are neglected.

Due to the susceptibility of conventional polymeric membranes to swell or dissolve in contact with organic solvents, NF applications are primarily confined to aqueous systems. A few studies, conducted with dilute aqueous solutions of methyl ethyl ketone, tetrahydrofuran and ethyl acetate, found onset of membrane swelling at feed concentrations above 8 % (Niwa et al., 1988). Solutions containing 20 % alcohol (such as ethanol, iso-propanol, and iso-butanol) yielded similar results (Oikawa et al., 1991). Very few studies have been conducted on organic solutions. Recent availability of solvent resistant NF membranes has led to the study of rejection characteristics of large molecules in organic solvents. Preliminary studies of the rejection behavior of certain dye molecules in methanol have indicated the dependence of solute rejection (as a function of permeate velocity) behavior similar to that predicted by the finely porous model (Whu et al., 2000). Effect of solvent properties on permeate flow through NF membranes also have been studied (Machado et al., 1999).

1.3.3 Applications

Since its first commercial application in the mid-1970s, NF has evolved to become a very versatile membrane separation technique, largely applied to process aqueous feed streams. Recent availability of solvent stable NF membranes (KOCH Membranes Bulletin, 1999) has made their application to process organic feed streams possible and it will not be long before their large-scale commercial applications in the pharmaceutical, fine chemicals and the chemical process industry become common.

Listed below are some of the commercial applications of NF technology:

1. *Water softening*: By far the largest users of NF technology are municipal drinking water plants. Operated at 70-100 psig, the NF membranes are able to reject 85-95 % of hardness and over 70 % of the monovalent ions (Watson et al., 1989). It is estimated that more than 100 million gallons per day of NF permeate is currently in design, construction or operation.
2. *Groundwater cleaning*: NF membranes are able to remove organics from industrial and agricultural effluents, which combine with chlorine to form trihalomethanes (THM), believed to be carcinogens (Amy et al., 1990). Existing plants in Florida are able to remove 97 % of the total organic halogens in potable water.
3. *Ultrapure water*: The electronics and semiconductor industry and certain medical and biotechnology applications require ultrapure water that is free of particulates and have total organic carbon (TOC) of less than 5 ppb. Whereas ion exchange membranes can bring down the TOC levels to about 30 ppb, negatively charged NF membranes have been employed to achieve the required goal of TOC less than 5 ppb (Ary et al., 1990).

4. *Beverage Industry*: NF is gradually replacing lime softening to achieve an industry standard of 50 ppm of alkalinity and also meet the federal THM limits (Paul, 1998).
5. *Industrial effluents*: Industrial wastewater containing precipitated hydroxides of heavy metals like nickel, iron, copper and zinc can be processed by NF to recover and reuse 90 % of the metals. Negatively charged NF membranes are used to remove negatively charge chromophoric organics (colored lignins and chlorinated lignins) from wash waters generated by the pulp and paper industry (Bindoff et al., 1987). Textile industries produce effluent water containing sodium hydroxide and organics. In a hybrid process, employed in South Africa, sodium hydroxide is first neutralized to form sodium chloride, processed through NF stages to recover the organics and consequently recovered as sodium hydroxide by electrochemical cells.
6. *Food Industry*: The dairy industry produce cheeses whey containing 4-6 % sodium chloride and 6% whey solids. With a biological oxygen demand of 45000 ppm, the whey poses a big waste disposal problem. NF membranes are now routinely used to reduce the whey solids to less than 1 %.

1.4 Diafiltration

Diafiltration is the process by which a membrane-based filtration process is used to rapidly and efficiently remove salts and/or lower molecular weight species from larger macromolecules (Porter, 1988). A diafiltration operation consists of three steps viz., pre-concentration, diafiltration and dilution. The diafiltration step can be carried out in a discontinuous or continuous mode. Figure 1.2 illustrates a schematic of the two modes of operation of a diafiltration process. As can be seen from the Figure 1.2, in continuous

diafiltration the solvent is added to the system at the same rate as permeate flux. Hence the volume and concentration of the rejected solute remains constant (assuming that the membrane rejection for the solute of interest is 100 %). Discontinuous diafiltration on the other hand involves alternate steps of concentration (via ultrafiltration or nanofiltration) and dilution (by solute-free solvent) until the desired reduction in the concentration of the salt (or any other small molecular weight solute) is achieved. A diafiltration operation requires the membrane to have a high rejection (~ 95 % +) for the larger solute molecules because the large convective flow through the membrane would otherwise wash out the solute of interest along with the smaller molecules.

UF membranes have been traditionally employed to carry out diafiltration operations. Concentration of enzymes (coupled with simultaneous reduction of salt concentration) (Porter, 1988) and albumin (coupled with simultaneous reduction of ethanol concentration) (Jaffrin et al., 1994) have been accomplished by ultrafiltration-diafiltration operation. Another process known as hemodiafiltration is carried out in a single membrane device known as a hemodiafilter. This device combines dialysis and hemofiltration to efficiently remove undesirable solutes from the feed (Ho and Sirkar, 1992). More recently diafiltration of industrially important dye solutions by nanofiltration also have been studied (Bowen et al., 1998). Research efforts on diafiltration have been confined to the study of aqueous feed solutions. Some optimization studies have shown that a combination of pre-concentration of the solution (to the desired final concentration) by ultrafiltration or nanofiltration followed by diafiltration (Asbi et al., 1991; Bowen et al., 1998) results in an optimum processing time.

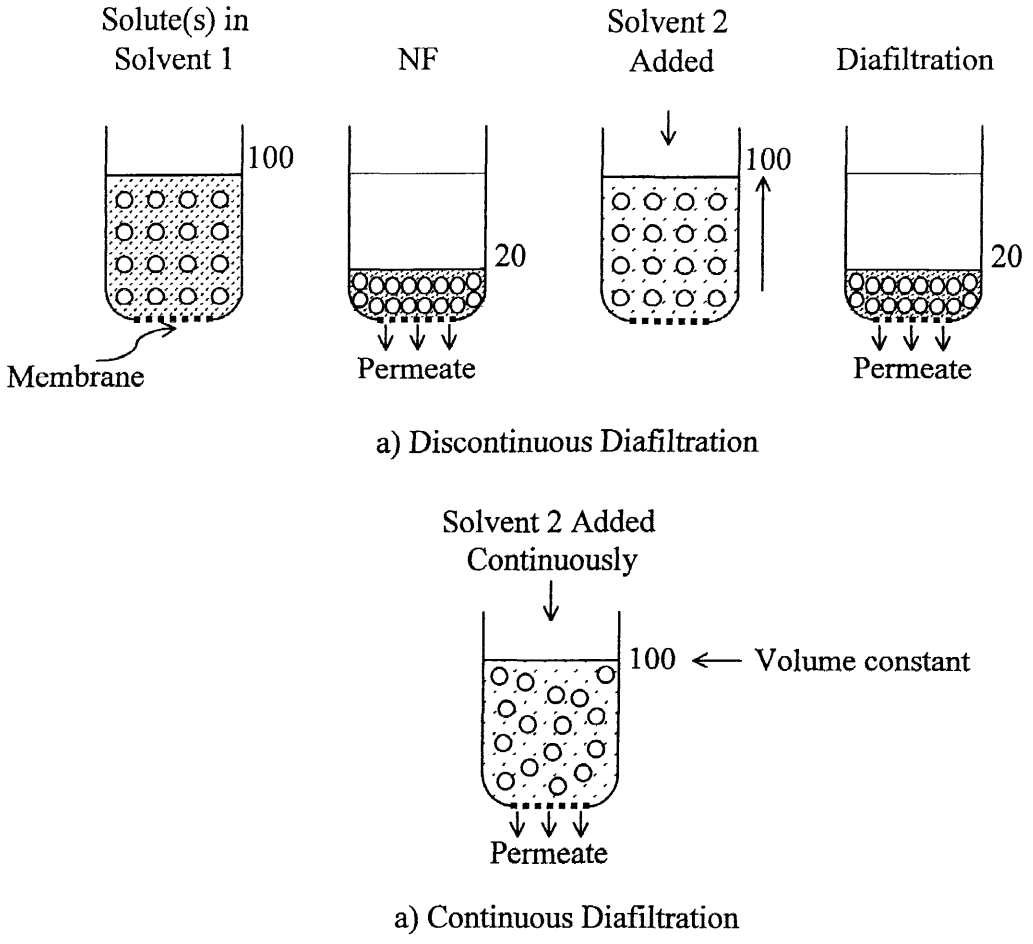

Figure 1.2 Schematic Representation of Discontinuous (a) and Continuous (b) Diafiltration (Asbi et al., 1991)

1.5 Research Problem and Thesis Objective

"If liquid-solid separations are membrane technology's present, its future lies in replacing such traditional unit operations as distillation and cryogenic applications" (Shanley, 1999). Most present day membrane-based commercial liquid-solid separations can only handle aqueous feed streams. However, many separation processes in the pharmaceutical, the fine chemicals and the chemical process industry in general, involve purely organic feed streams that must be processed to separate components of interest. Recent availability of solvent stable nanofiltration membranes has made it possible to process pure organic solutions, but extensive research efforts are required before such membranes can be offered as a viable alternative to conventional separation processes.

Organic synthesis of bulk drugs generally involves multi-step reactions where each reaction may be carried out in a different solvent medium. Most reactor streams contain a thermally labile, high molecular weight (>250-1000 daltons) product of interest along with other smaller molecular weight by-products. The product (intermediate or final) must be separated from other by-products and also the solvent medium, because quite often the subsequent reaction (carried out in a different solvent medium) cannot tolerate the original solvent as an impurity beyond a certain concentration. Conventional separation processes require special conditions to handle thermally labile products and sometimes require extraneous chemicals (which are a potential source of environmental pollution) to effect separation. Nanofiltration membranes, on the other hand, can selectively retain solutes with molecular weight greater than 250 daltons and simultaneously allow the smaller molecules to wash out along with the solvent. Furthermore, they can achieve these twin objectives at ambient temperatures. Hence, it is

the objective of this thesis to explore the feasibility of solvent stable nanofiltration membranes in carrying out solvent exchange via discontinuous diafiltration process for an industrially relevant system. Furthermore, the behaviors of the permeate flux and solute rejection profiles during nanofiltration and diafiltration are also to be studied.

1.6 Choice of Model System

Erythromycin is chosen as a solute of interest as it is a commercially relevant and widely used broad-spectrum macrolide antibiotic. Moreover, the solubility of erythromycin in both methanol and ethyl acetate is at least 20 wt % at room temperature. In order to carry out solvent exchange, the original solvent and the replacement solvent must be completely miscible with each other. Transport of solvents forming an immiscible mixture, would be highly dependent upon the stirring conditions inside the cell and the permeate concentration thus obtained would not be reliable. Methanol and ethyl acetate are completely miscible with each other at room temperature and are widely used solvents in the pharmaceutical industry (Chung, 1996).

CHAPTER 2

TRANSPORT MODEL

NF membranes are a new class of thin film composite membranes, made by interfacial polymerization on polysulfone or polyamide ultrafiltration membranes (Wang et al., 1997). As discussed earlier, their separation mechanisms involve both steric effects and electrical effects. The average pore diameter of most NF membranes is of the order of 2 nm (Raman et al., 1994). Due to the small pore diameter, molecular size is an important parameter for modeling of the retention of organic molecules. Although comparison of hydrodynamic volume gives satisfactory prediction between different classes of molecules for UF membranes, the much smaller pore sizes of NF membranes require the stronger interactions between the pores and the solutes to be accounted for. Preliminary studies on pure organic systems of methanol-dye solutions have suggested the possibility that the *finely porous model* (which takes into account the friction forces between solute molecules and the membrane) may predict the solute rejection as a function of permeate flux through uncharged NF membranes (Whu, et al. 2000). The model will be briefly discussed in this chapter.

Due to the lack of solvent-stable NF membranes, most experimental and theoretical studies have been limited to aqueous systems. However, some attempts have been made to describe the solvent flux in organic systems. These studies use a modified Poiseuille expression (*viscous approach*) (Nguyen et al., 1979) or a modified solution diffusion model (*solubility approach*) (Reddy et al., 1996). A generalized model, which combines these two approaches, has also been proposed (Urugami et al., 1979). However, these models do not take into account solvent properties and solvent-membrane

interactions to predict permeate flux. The Machado-Hasson-Semiat (MHS) model (Machado et al., 1999) uses a resistance in series like concept to predict solvent flux through a composite NF membrane. Solvent properties (such as viscosity and surface tension) that affect the permeate flux through the membrane (Machado et al., 1999) have been accounted for in this model. It will be discussed in detail in this chapter.

The extended Nernst-Planck equation forms the basis for the description of the transport of charged and uncharged solute molecules inside porous membranes. They will be briefly discussed in this chapter.

2.1 Permeate Flux through NF Membranes

2.1.1 Finely Porous Model

The finely porous model, developed by Merten (1966) assumes that the porous membrane has properties intermediate to those of solution-diffusion membranes and viscous flow membranes. It incorporates a frictional force term in to the pressure gradient across the membrane. The friction term affects not only the solute permeability of the membrane but its apparent hydrodynamic permeability as well. Solvent properties and solvent-membrane interactions are not accounted for. The model assumes perfectly cylindrical pores and a fully developed parabolic velocity profile within the pores. Hence the permeate flux, J_s, generally expressed as,

$$J_S = \frac{L_P}{\tau\delta}(\Delta P - \Delta\Pi) \tag{2.1}$$

when modified to include the friction factor between the solute and the membrane becomes,

$$J_S = \frac{L_P'}{\tau\delta}(\Delta P - \Delta\Pi) \tag{2.2}$$

where the apparent permeability, L_p' is defined as,

$$J_S = \frac{L_P}{\tau\delta}\left[\frac{1}{1+\frac{L_P f_{im} C_{ip}}{\varepsilon}}\right](\Delta P - \Delta\Pi) \tag{2.3}$$

Here the membrane permeability, L_P, defined by the Hagen-Poiseuille equation is,

$$L_P = \frac{\varepsilon r_P^2}{8\eta} \tag{2.4}$$

As evident from equation 2.3, the apparent permeability, L_p', is always lower than the membrane permeability, L_P. When the friction coefficient, f_{im}, between the solute, i, and the membrane is negligible the apparent permeability, L_p', equals the membrane permeability, L_P.

2.1.2 Machado-Hasson-Semiat (MHS)Model

The MHS model assumes a composite NF membrane to contain three main layers; a NF top skin, an intermediate UF layer, and a baser support layer. As illustrated in Figure 2.1, there are three resistances in series: R_S^0 (surface resistance at the pore entrance), which accounts for the resistance generated due to the difference in the surface energy between the solvent molecules and the polymer membrane surface, R_μ^1 (viscous resistance during flow through the NF skin portion of the pore), and R_μ^2 (viscous resistance during flow through the UF portion of the pore). The resistance of the porous support layer is assumed to be negligible.

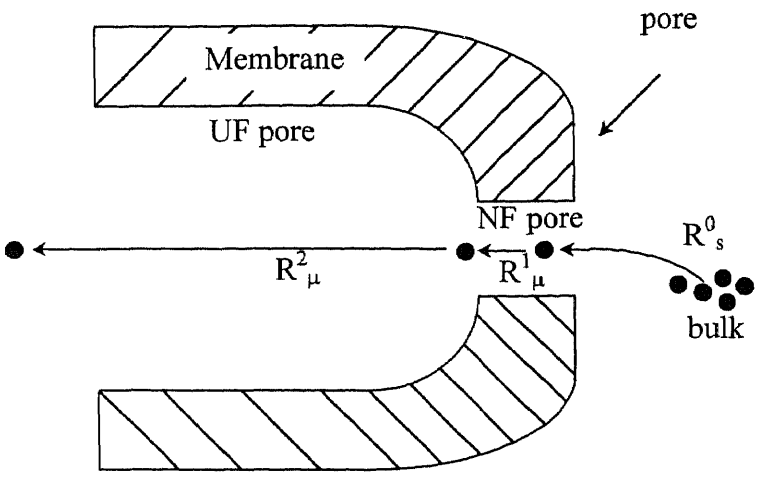

Figure 2.1 Schematic Representation of the Three Flow Resistances in the Transport Path of a Solvent Through a Composite NF Membrane (Machado, et al., 1999)

Based on these assumptions the solvent flux through membrane is given by,

$$J_S = \frac{\Delta P}{R_S^0 + R_\mu^1 + R_\mu^2} \tag{2.5}$$

where,

$$R_S^0 = \frac{k_M^0}{\left(d_p^1\right)^2}(\gamma_M - \gamma_S) \tag{2.6}$$

$$R_\mu^1 = k_M^1 \frac{\mu}{\left(d_p^1\right)^2} \tag{2.7}$$

$$R_\mu^2 = k_M^2 \frac{\mu}{\left(d_p^2\right)^2} \tag{2.8}$$

The surface resistance, R_S^0, is directly proportional to the difference in the surface tension of the membrane, γ_M, and the solvent, γ_S, and inversely proportional to the square of the pore diameter, d_p^1, of the NF skin. The proportionality constant, k_M^0, describes the pore characteristics of the membrane. The viscous resistances, R_μ^1 and R_μ^2, are directly

proportional to the solvent viscosity, μ, and inversely proportional to the square of the pore diameters of the NF skin, d_p^1, and the UF layer, d_p^2, respectively. Constants, k_M^1 and k_M^2, take into account the porosity and tortuosity of the membrane layers. Substitution of equations (2.6), (2.7), and (2.8) in equation (2.5) yield,

$$J_S = \frac{\Delta P}{\varphi[(\gamma_M - \gamma_S) + f_1\mu] + f_2\mu} \tag{2.9}$$

Equation (2.9) consists of three parameters; two solvent independent parameters, f_1 (characterizing the NF skin) and f_2 (characterizing the UF layer), and one solvent parameter, φ, which are defined as follows,

$$f_1 = \frac{k_M^1}{k_M^0} \tag{2.10}$$

$$f_2 = \frac{k_M^2}{\left(d_p^2\right)^2} \tag{2.11}$$

$$\varphi = \frac{k_M^0}{\left(d_p^1\right)^2} \tag{2.12}$$

This model not only accounts for the varying membrane properties of the various layers of the composite NF membrane but also contains the solvent properties (especially surface tension) and the solvent-membrane interaction as variables. Studies on nanofiltration of solvent mixtures of acetone with C_1-C_5 alcohols through MPF-50 membrane showed that equation (2.9) closely predicts the solvent flux for a given solvent mixture. However, for systems where the surface tension of the solvent mixture was much higher than that of the membrane led to a negative value of φ, which would result

in a lower permeate flux with increasing transmembrane pressure difference. This is a clear deficiency of the model. Studies on acetone paraffin (pentane and hexane) mixtures showed that the flux was not a monotonous function of concentration as opposed to that predicted by equation (2.6). Modification of the equation by accounting the dielectric effects gave a reasonable fit, but detailed study of dielectric effects is required to get a clear picture. Furthermore, this semi-empirical model, developed for solvent mixtures, needs to be modified to account for solute-solvent interactions if it is to predict the flux of solute-mixed solvent systems.

2.2 Transport of Solute through NF Membrane

The extended Nernst-Planck equation describes the transport of solute molecules inside the membranes. It accounts for the solute flux due to diffusion, convection and electric field gradient and is given by,

$$J_i = -D_e \frac{dC_{im}}{dx} + K_{ic} C_{im} J_S - \frac{z_i C_{im}}{RT} F \frac{d\psi}{dx} \tag{2.13}$$

The above equation takes the finely porous model into account by using the effective diffusion coefficient, D_e (which is the diffusion coefficient through large pores reduced by the hindrance factor for diffusion, K_{id}), given by,

$$D_e = K_{id} D \tag{2.14}$$

K_{ic} accounts for the hindrance factor for convection and includes the friction forces generated between the solute and membrane and between the solute and solvent.

2.2.1 Uncharged Solutes

For uncharged solutes, in the absence of any electrical field effects, equation (2.13) becomes

$$J_i = -D_e \frac{dC_{im}}{dx} + K_{ic} C_{im} J_S \tag{2.15}$$

Solute rejection, R, can be determined by integration of equation (2.15) with appropriate boundary conditions ($C_{im}(0) = k' C_{ir}$ and $C_{im}(\tau\delta) = k'' C_{ip}$) and the assumption that $J_i (= J_s C_{ip})$, J_s, D_e, and K_{ic} are constant and purely steric interactions exist. Hence,

$$R = 1 - \frac{C_{ip}}{C_{ir}} = 1 - \frac{K_{ic}\phi}{1 - \exp(-Pe_m)[1 - K_{ic}\phi]} \tag{2.16}$$

where, ϕ (partition coefficient) and Pe_m (Peclet number) are defined as,

$$\phi = \left(1 - \frac{r_i}{r_p}\right)^2 \tag{2.17}$$

$$Pe_m = \frac{\tau\delta}{\varepsilon} K_{ic} \frac{J_s}{D_e} \tag{2.18}$$

Hence the rejection at a given permeate flux, J_s, is a function of two parameters, namely $\tau\delta / \varepsilon$ and r_i / r_p (ratio of solute radius to pore radius).

2.2.2 Charged Solutes

The extended Nernst-Planck equation in its entirety is used to define the transport of charged species. Conditions of electroneutrality in the bulk solution and inside the membrane are assumed. Also, solvent dielectric effects on ion partitioning are not taken into account. Equations (2.19), (2.20), and (2.21) describe the conditions of

electroneutrality in the bulk solution, inside the membrane and the zero current conditions within the membrane respectively.

$$\sum_{i=1}^{n} z_i C_i^0 = 0 \tag{2.19}$$

$$\sum_{i=1}^{n} z_i c_i = -X \tag{2.20}$$

$$\sum_{i=1}^{n} F(z_i J_i) = 0 \tag{2.21}$$

To determine the concentration just inside the membrane, at the membrane-bulk solution interface, the Donnan and steric effects are taken in to account to give the following equilibrium condition,

$$\frac{\gamma_{im} C_{im}}{\gamma_i^0 C_i^0} = \phi \exp\left(-\frac{z_i F}{RT} \Delta\psi_D\right) \tag{2.22}$$

where, γ_i is the activity coefficient, $\Delta\psi_D$ is the Donnan Potential, F is the Faraday constant, C_i^0 is the concentration of ion, i, in the external solution, and C_{im} is the ion concentration in the membrane. A detailed study on the transport model of charge solutes can be found elsewhere (Merten, 1966; Bowen et al., 1999).

2.3 Diafiltration

Diafiltration can be carried out in a discontinuous or a continuous mode. Optimization studies of a diafiltration process have concentrated on two parameters, the treatment time (Asbi et al., 1994; Cheryan et al., 1991; Bowen et al., 1998) and the membrane area (Dutre et al., 1994). These studies have found that the shortest processing time is achieved by operating at the maximum allowable solute (of interest) concentration during

the diafiltration step. This can be achieved by a pre-concentration step via NF. The primary objective of these studies was to reduce the concentration of a small molecule (e.g. sodium chloride, ethanol, etc.) by carrying out diafiltration with water as the diluent. However, in the context of the present work, it is essential to determine the change in the concentration of the original solvent (in the retentate) over the period of the diafiltration.

Consider continuous diafiltration (solvent exchange) of a pre-concentrated solution, containing a large solute (MW > 300) of interest and smaller solute(s) (MW <<300) in an organic solvent, by the addition of a second solvent. Assuming that the NF membrane completely rejects the solute of interest and exhibits no selectivity for the solvent mixture or the smaller solute(s) molecules, we get for zero accumulation (V = constant),

$$V\frac{d\bar{V}_{so}}{dt} = -\frac{\bar{V}_{so}}{\bar{V}_{so}+\bar{V}_{sr}}A_m J_{sm} \tag{2.23}$$

where, $$\bar{V}_{so}+\bar{V}_{sr}+\bar{V}_{l}=1 \tag{2.24}$$

Equations (2.23) and (2.24) assume a perfectly mixed feed solution. In the above equation, the term $\bar{V}_{so}$ (volume fraction of original solvent in the membrane cell) accounts for the original solvent and also the small molecular weight solutes, which are completely washed out. Similarly, the term $\bar{V}_{l}$ (volume fraction of the large molecular weight solute) accounts for the large molecular solute of interest that is present in the original solution and also any new large molecular weight reactants (for the next reaction step in multi-step organic synthesis) that are added along with the replacement solvent. $\bar{V}_{sr}$ is the volume fraction of the of replacement solvent in the membrane cell.

CHAPTER 3

MATERIALS AND METHODS

3.1 Chemicals and Gases Used

Erythromycin, $C_{37}H_{67}NO_{13}$, FW 733.9, approx. 98%, (Sigma Chemicals, St. Louis, MO); methanol, CH_4O, FW 32.04, HPLC grade, (Fisher Scientific, Fair Lawn, NJ); ethyl acetate, $C_4H_8O_2$, FW 88.11, Optima grade, (Fisher Scientific, Fair Lawn, NJ); ethyl alcohol denatured, (Fisher Scientific, Fair Lawn, NJ); sulfuric acid, H_2SO_4, FW 98.08, NF / FCC grade, (Fisher Scientific, Fair Lawn, NJ); sodium metabisulfite, $Na_2S_2O_5$, FW 190.1, 98.8%, (Sigma Chemicals, St. Louis, MO); glycerol, $C_3H_8O_3$, FW 92.09, 99%, (Sigma Chemicals, St. Louis, MO); benzalkonium chloride, 50 wt % aqueous solution, (Acros Organics, Pittsburgh, PA); and nitrogen compressed, N_2, extra dry, (Matheson Gases and Equipment, East Rutherford, NJ).

3.2 Membranes

SelRO® chemically stable flat sheet membranes for nanofiltration industrial applications, manufactured by Koch Membrane Systems, Wilmington, MA, were used. The membranes were supplied as 8.5″ wide by 11″ long sheets soaked in their preserving solution and enclosed in individual plastic envelopes. MPF-50 and MPF-60 solvent stable nanofiltration membranes were used. As specified by the technical data sheets supplied by the manufacturer, the membranes were tested for solvent stability by immersion in organic solvents for 125 hours at 25°C. Depending upon the state of the membrane at the end of the test, the membranes were characterized as stable (S), limited stability (LS) and not stable (NS). The membranes were tested for a wide variety of polar and non-polar

solvents, such as alcohols, esters, ketones, alkyl halides, alkanes, etc., over a pH range of 2-10.

The membranes were stable in most of the solvents; however, in extremely polar solvents like dimethylformamide, dimethylsulfoxide or dimethlyacetamide the membranes exhibited limited stability or no stability depending on the water concentration. Some of the properties of the membranes, as specified by the manufacturer, are summarized in Table 3.1. The membranes were characterized by two important properties, namely, molecular weight cut-off (MWCO) and hydrophobic or hydrophilic nature of the membrane.

Table 3.1 Properties of the Solvent Stable NF Membranes

Type	MWCO (daltons)	pH range (solvent/water applications)	Nature	Operating Conditions	
				Temp. (°C)	Press. (psi)
MPF-50	700	4 – 10	Hydrophobic	40 (Max.)	514 (Max.)
				30 (Rec.*)	440 (Rec.*)
MPF-60	400	2 – 10	Hydrophobic	40 (Max.)	585 (Max.)
				30 (Rec.*)	440 (Rec.*)

* Recommended by manufacturer

A MWCO of 700 daltons (for MPF-50) membrane means that the membrane rejects at least 95.0 % of molecules with a molecular weight of 700 or more. Hence, as seen from Table 3.1, MPF-60 membrane is tighter than MPF-50. As indicated by the manufacturer, the test solution for nanofiltration was to contact the active side of the

membrane, which was shiny and smooth. MPF-50 was supplied in a preserving solution of 0.1 % sodium metabisulfite and 10.0 % glycerin whereas MPF-60 was preserved in 20.0 % glycerin and 0.7 % benzalkonium chloride. The manufacturer recommended the storage of these membranes in the respective preserving solution in a dry, cool area at a temperature ranging from 4°C to 30°C.

3.3 Membrane Cell

A Sepa® ST, model 56414, high-pressure, low hold-up volume stirred test cell, supplied by Osmonics, Minnetonka, MN, was used to conduct experimental runs in the present thesis. The material of construction of the membrane cell, SS 316 L, made it resistant to most chemical degradation. A schematic of the membrane cell is given in Figure 3.1. The membrane cell consisted of a cylindrical SS 316 L body having a processing volume of 300 mL. At the top end of the cell, it was connected to the pressurization assembly by means of a high pressure coupling capable of operation at a maximum pressure of 1000 psig (6.89 MPa). A similar high pressure coupling connected the membrane cell to the membrane support assembly at the bottom end of the cell. A flat, circular membrane having a diameter of 4.9 cm and an effective membrane area of 15.2 cm^2 was supported on a 1/16″ thick circular 20 μm porous support disc. A hold-up volume of 1 mL remained underneath the porous support. A Teflon® coated stirring bar, suspended inside the membrane cell, stirred the cell contents. A custom made 2″ long, 1/8″ diameter SS tube facilitated permeate collection. The wetted sealing parts, such as O-rings and gaskets were made of ethylene propylene to ensure resistance to methanol. A 1/4″ pressure inlet at the top of the membrane cell facilitated the pressurization of the membrane cell.

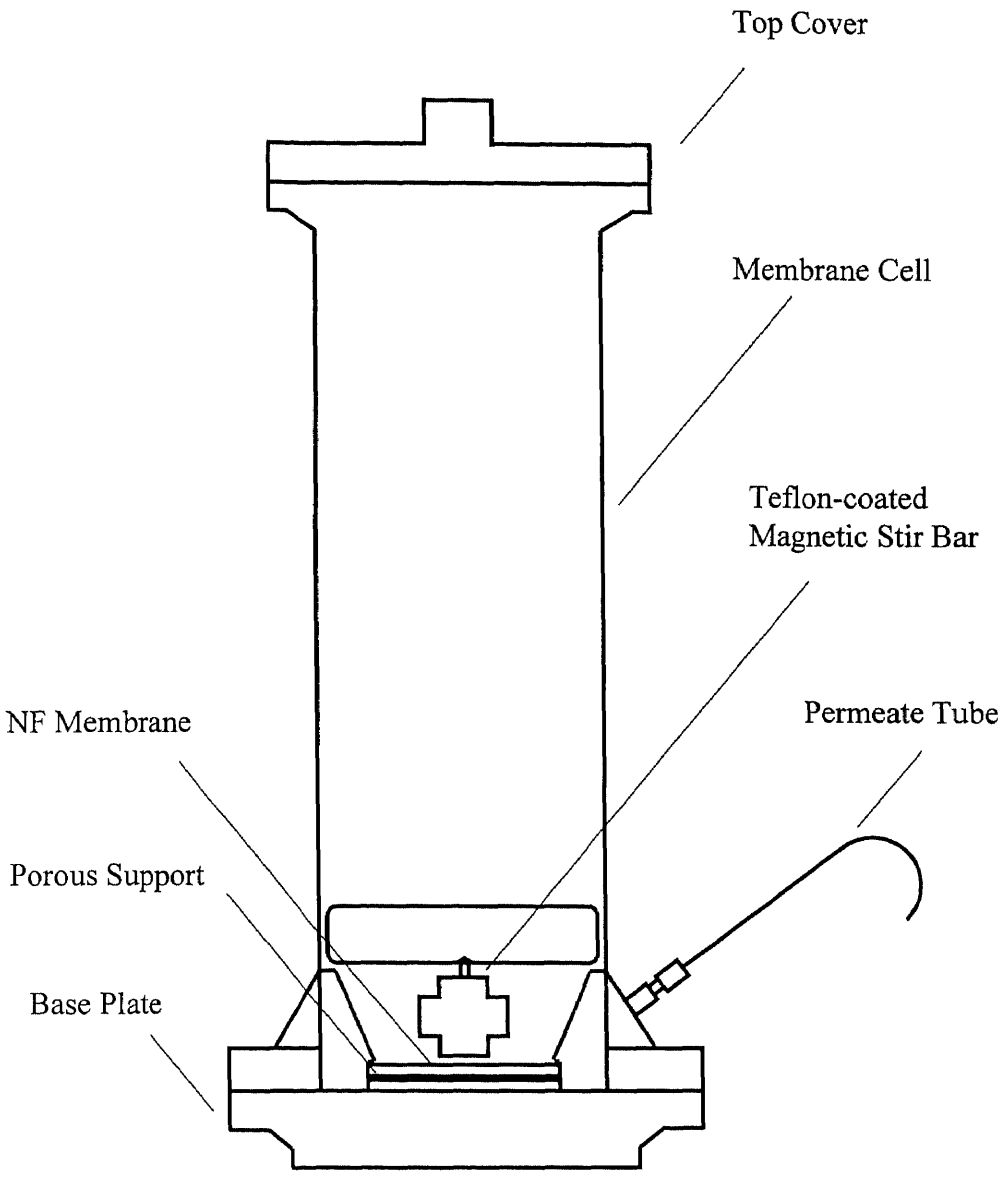

Figure 3.1 Schematic Diagram of the Membrane Cell

3.4 Experimental Set-up

A schematic of the laboratory setup is given in Figure 3.2. It consisted of a Sepa® ST membrane cell (described above) coupled to a membrane support assembly by means of a high pressure coupling. At the other end of the cell the pressure inlet was connected to a compressed nitrogen cylinder by means of a 1/4″ S.S. tubing. The pressure within the membrane cell was monitored by means of pressure gauges mounted on a single stage pressure reducing valve near the nitrogen cylinder outlet and near the membrane cell inlet. For safety considerations an adjustable relief valve (R. S. Crum, Mountainside, NJ), set at 470 psig (3241 kPa) was installed in the set-up piping. A system of ball valves, check valves and a pressure regulator (Matheson Gases and Equipment, East Rutherford, NJ) was also installed in conjunction with the relief valve. The assembly was used in the depressurization of the membrane cell. The membrane cell was mounted on a variable speed magnetic stirring plate (Corning Corp., Budd Lake, NJ).

3.5 Experimental Procedure

3.5.1 Membrane Conditioning

Nanofiltration flat sheet membranes were supplied soaked in their preserving solutions. Removal of the preserving solution and membrane activation was essential to preparing the membrane for regular experimental work. As a first step, a circular piece of membrane was cut from the sheet and was rinsed thoroughly with deionised water to remove bulk of the preserving solution. The membrane was then immersed in deionised water overnight to ensure complete removal of the preserving solution. Membrane activation was carried out in the membrane cell by flushing it with ethanol at 440 psig

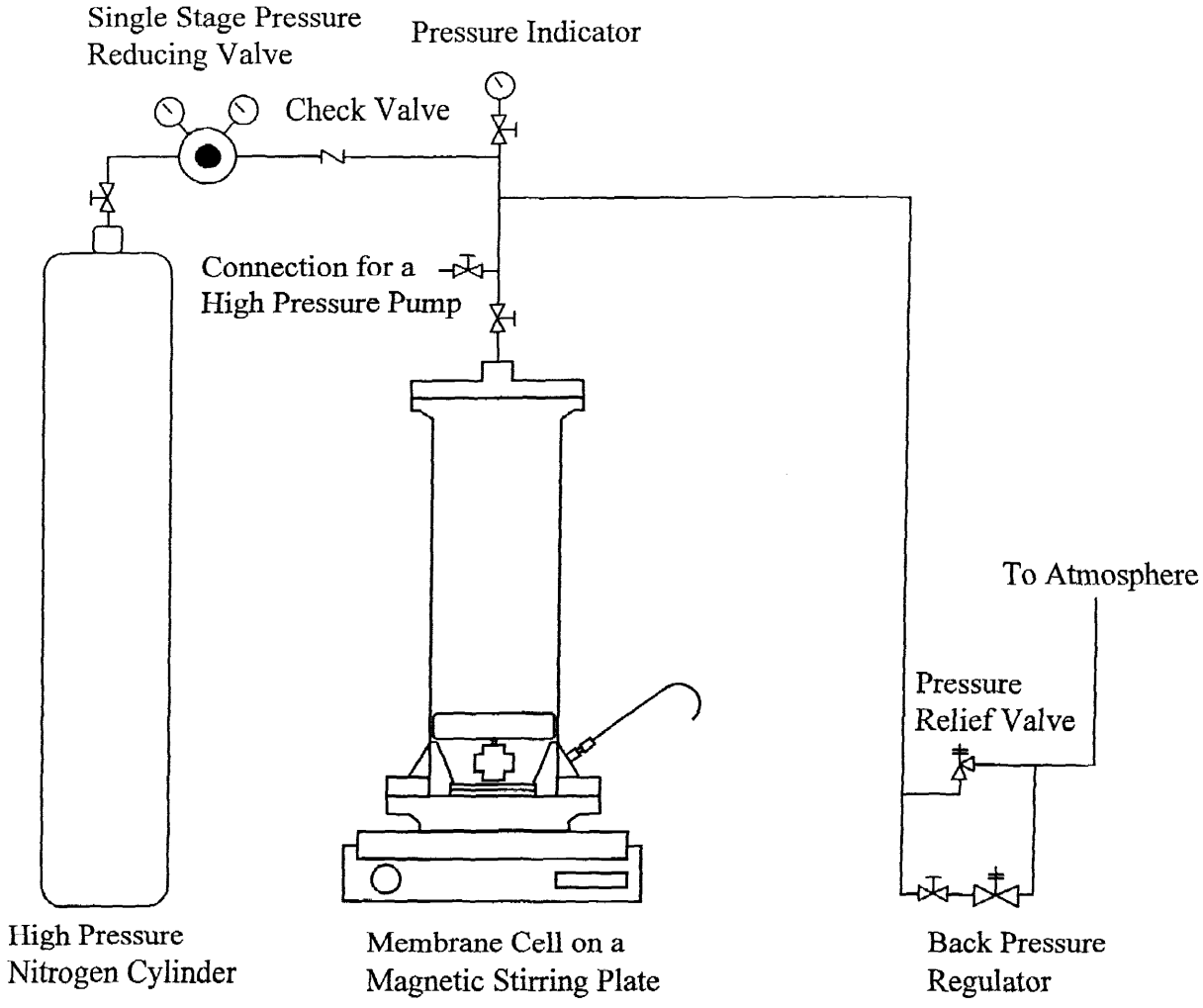

Figure 3.2 Schematic Diagram of the Laboratory Set Up

(3033.8 kPa) and room temperature. Activation was carried out long enough (approximately 80–100 minutes) to collect at least 10 mL of permeate. As recommended by the membrane manufacturer (Koch Membrane Systems, Wilmington, MA), the activated membranes that were to be used for nonaqueous organic solvent applications were stored in ethanol.

3.5.2 Nanofiltration with Pure Solvents

Conditioned membranes were used to gather the pure solvent permeation data. A membrane sample was loaded in the membrane cell and subsequently, approximately 200 mL of the solvent were added to the cell. The tests were then carried out at 440 psig (3033.8 kPa) and at room temperature under stirred conditions. Permeate samples were collected in graduated 25 mL glass cylinders at regular intervals. Nanofiltration experiments with pure solvents were conducted for MPF-50 and MPF-60 membranes at 440 psig (3033.8 kPa) and room temperature with methanol and ethyl acetate respectively.

At the end of each test run, the nitrogen supply to the membrane cell was stopped. Depressurization of the system was carried out gradually using the back pressure regulator assembly. A gradual drop of approximately 50 psi/min prevented the solvent in the membrane cell from flashing and contaminating the pressure delivery tubing. Another consideration in the gradual pressure reduction was the need to maintain the compacted state of the membrane that it had achieved following the test run. Solvent flux profile over several test cycles of pressurization and depressurization was thereby obtained. Used membranes were preserved for future tests by keeping them soaked in ethanol.

3.5.3 Nanofiltration and Diafiltration with Solutions

Nanofiltration and diafiltration experiments for solutions and mixed solvents respectively, were carried out in a manner similar to that for pure solvent runs. Sections 3.5.3.1 and 3.5.3.2 describe the differences in experimental procedures.

3.5.3.1 Nanofiltration of a Given Solution: Solution of erythromycin in ethyl acetate was prepared by dissolving a known amount of erythromycin in ethyl acetate in a 200 mL volumetric flask. The solution concentration of erythromycin was determined by using a Hitachi U2000 spectrophotometer after appropriate dilution and color development of the test sample. Section 3.6.1 provides the details of the analytical procedure for determining erythromycin concentration.

To carry out a nanofiltration run, a conditioned membrane was loaded into the membrane cell. The cell was then placed on the magnetic stirring plate and the Teflon coated magnetic bar inside the cell was rotated at a fixed speed. The membrane cell was then pressurized by nitrogen gas up to 440 psig (3033.8 kPa). Permeate samples were collected in 25 mL graduated volumetric cylinders at regular intervals. The permeate samples were analyzed for erythromycin concentration after appropriate dilution and color development. In a typical nanofiltration run, 200 mL of feed having a pre-determined erythromycin concentration was prepared; of the 200 mL solution, 190 mL were charged into the membrane cell and concentrated up to about 40 mL. The remaining 10 mL of feed were used for concentration analysis. The average of the absolute value of the difference between the concentrations determined spectrophotometrically and gravimetrically was less than 1.0 %. Permeate sampling was done more frequently at the

beginning of a run so as to get accurate information about the initial membrane compaction behavior. Permeate flux was calculated in terms of L/m^2h and the observed rejection, R, was determined by performing a mass balance on erythromycin. Detailed flux and observed rejection calculation procedures can be found in Appendix A.

Nanofiltration experiments were done with erythromycin in ethyl acetate solution, using MPF-50 and MPF-60 membranes at 440 psig (3033.8 kPa) and room temperature. A starting feed concentration of 5000 μg/mL was used in all tests so as to get a uniform basis for performance comparison of both the membranes. The initial feed volume was reduced to approximately 40 mL. Further reduction in solution volume within the membrane cell would result in a significant increase in the solution concentration, giving rise to considerable concentration polarization. Upon completion of the test, the membrane cell was depressurized gradually taking the same precautions as described in section 3.5.2. Membrane samples were then stored in ethanol and the membrane cell, along with all accessories were thoroughly cleaned and stored in a dust free environment.

3.5.3.2 Diafiltration: A membrane subjected to a nanofiltration run as described in section 3.5.3.1 was used for diafiltration experiments. Diafiltration was conducted in a manner similar to a nanofiltration experiment. A conditioned membrane subjected to nanofiltration was loaded into the membrane cell, which was then mounted on a magnetic stirring plate so as to enable the retentate to be stirred continuously. Approximately 20 mL solution of erythromycin in ethyl acetate, subjected to a nanofiltration experiment was mixed with 80 mL of pure methanol to give an approximately 20 % ethyl acetate solution. A small quantity of this feed solution was used to analyze the erythromycin

concentration (analysis detail in section 3.6.1) and ethyl acetate concentration (analysis details in section 3.6.2).

The feed solution was then pressurized to 440 psig (3033.8 kPa) and permeate samples were collected in 25 mL graduated volumetric cylinders. Permeate samples were collected more frequently at the beginning of the experiment so as to get accurate information about the initial membrane compaction behavior. Each permeate sample was analyzed for the concentrations of erythromycin and ethyl acetate. Based on the results obtained from the concentration analysis, the observed rejection pattern of the membrane during the diafiltration stage was collected. The diafiltration run was continued till the volume of the retentate was reduced to the original erythromycin and ethyl acetate solution volume, i.e. approximately 20 mL. The retentate was also analyzed for erythromycin and ethyl acetate concentration. This solution of erythromycin in ethyl acetate and methanol was again diluted with pure methanol to approximately 4 % ethyl acetate. This solution was then subjected to another cycle of diafiltration. During this cycle, permeate samples were collected and analyzed in a manner similar to that in the previous diafiltration run. Depressurization of the membrane cell at the end of each diafiltration run was done gradually, taking the same care as with the nanofiltration experiment.

A membrane sample, after activation, was subjected to three cycles, one nanofiltration cycle and two diafiltration cycles. Figure 3.3 is a schematic showing the pressurization, activation/nanofiltration/diafiltration and depressurization cycles employed for each membrane tested.

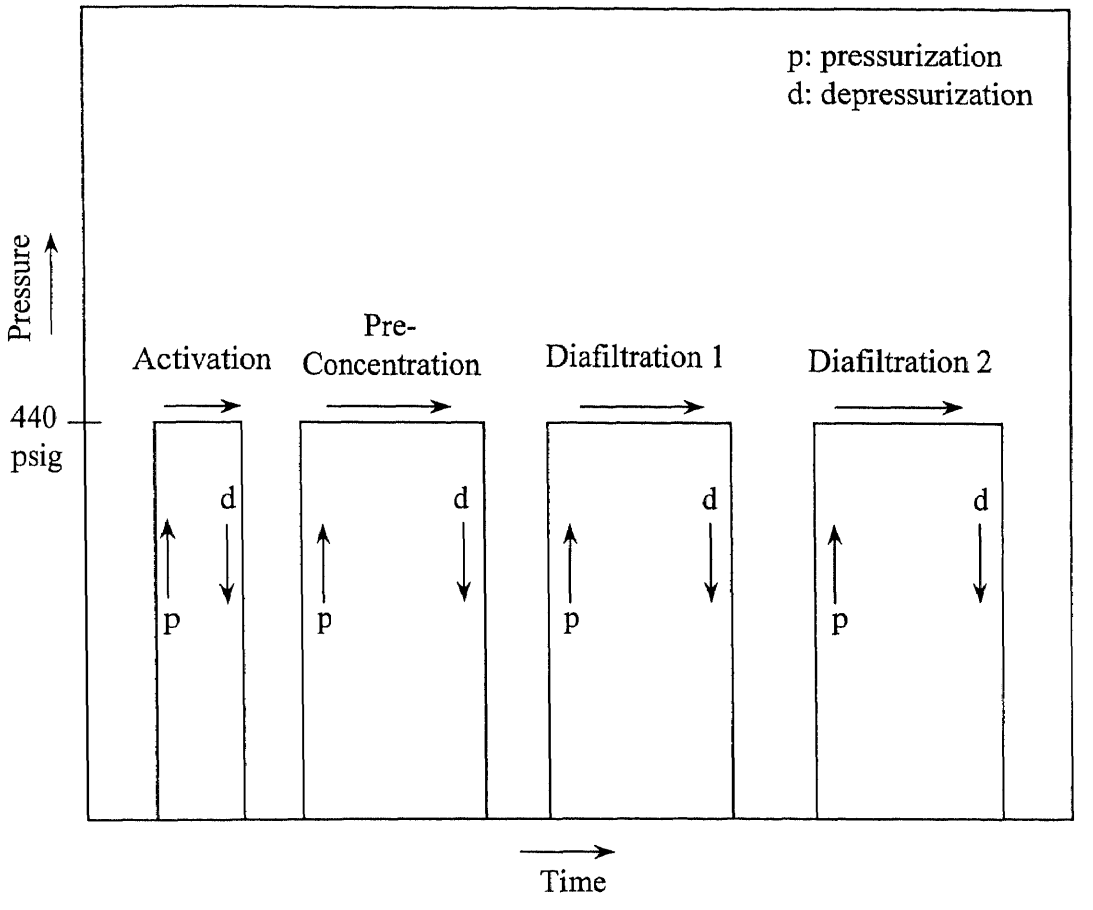

Figure 3.3 Schematic Showing the Pressurization, Activation/Nanofiltration/Diafiltration and Depressurization Cycles

3.6 Analysis of Compositions of Feed, Permeate and Retentate Samples

3.6.1 Analysis for Erythromycin

Concentrations of the feed, permeate and retentate solutions were determined using a Double Beam UV/Vis spectrophotometer, model U2000 (Hitachi Instruments, Danbury, CT). The solution of erythromycin in methanol or ethyl acetate is colorless. Due to this the calibration curve in the very dilute concentration range of 100 μg/mL or less is not very accurate. Also, for identical concentrations of erythromycin in methanol and ethyl acetate respectively, the absorbance of each sample is different. This would require separate calibration curves for pure methanol, pure ethyl acetate and their mixtures thereof. To avoid the need for such multiple calibration curves and to get an accurate calibration curve, especially in the very dilute concentration range, each sample to be analyzed was diluted with deionised water such that the concentration of the organic phase was less than 5.0 % by volume. This was required because the solubility of ethyl acetate in water at room temperature is less than 8.0 % (CRC Handbook, 1998). The dilute sample was then mixed with 10 mL of 5 M sulfuric acid and heated to 100 °C in a water bath for 2 minutes to develop color in the solution. The solution was then cooled, further diluted with sulfuric acid to 25 mL and analyzed for absorbance. This analysis method was adopted from (Chen et al., 1993).

Absorbances of samples prepared in this way, either in methanol or ethyl acetate showed no difference in their absorbance values. Hence only a single calibration curve sufficed for the entire concentration range of methanol and ethyl acetate solution. Figure 3.4 shows a flowchart for the dilution technique employed for the erythromycin concentration analysis. Figure 3.5 shows the calibration curve used to determine the

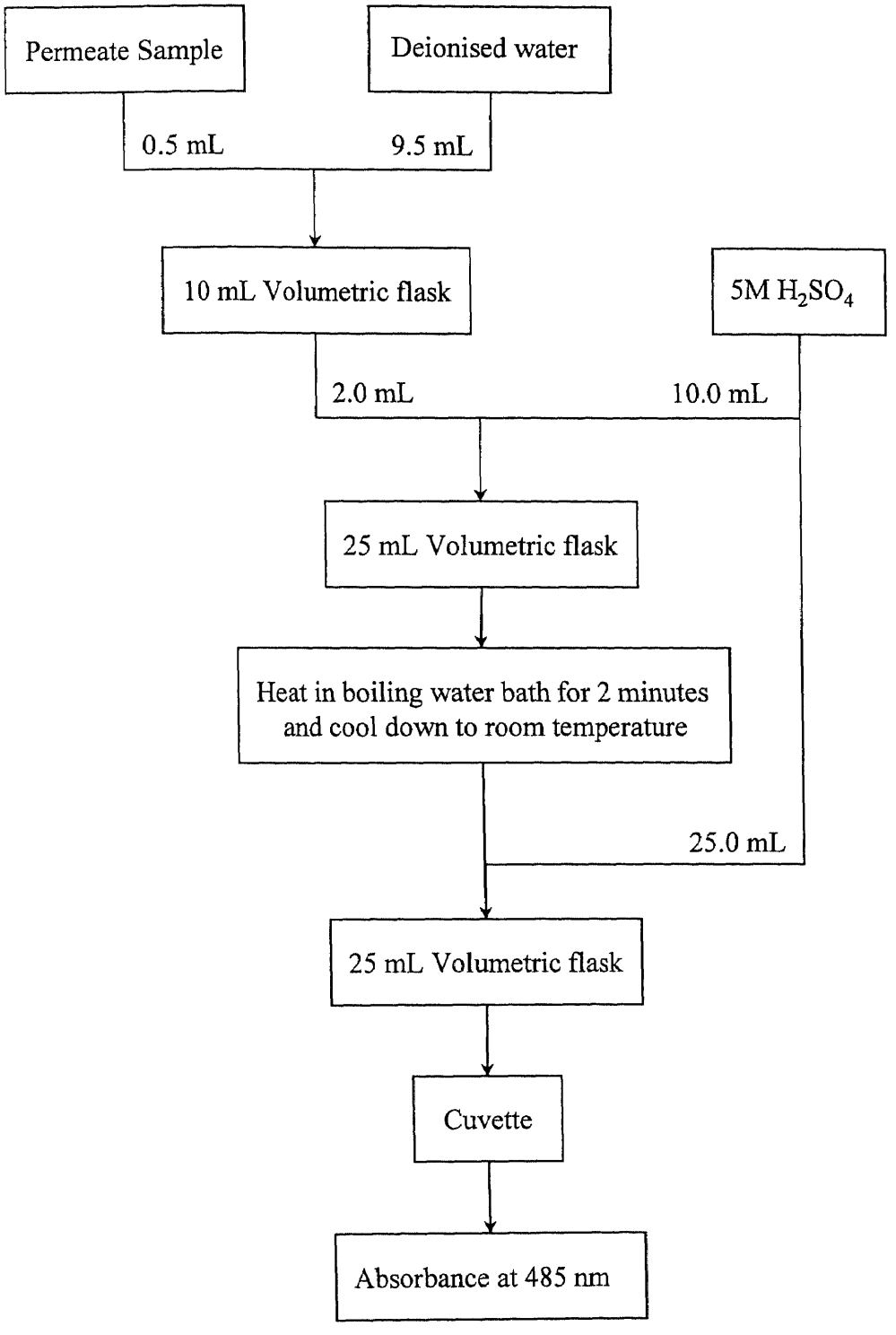

Figure 3.4 Flowchart Depicting the Method Employed to Determine Erythromycin Concentration in Ethyl Acetate, Methanol and their Mixtures

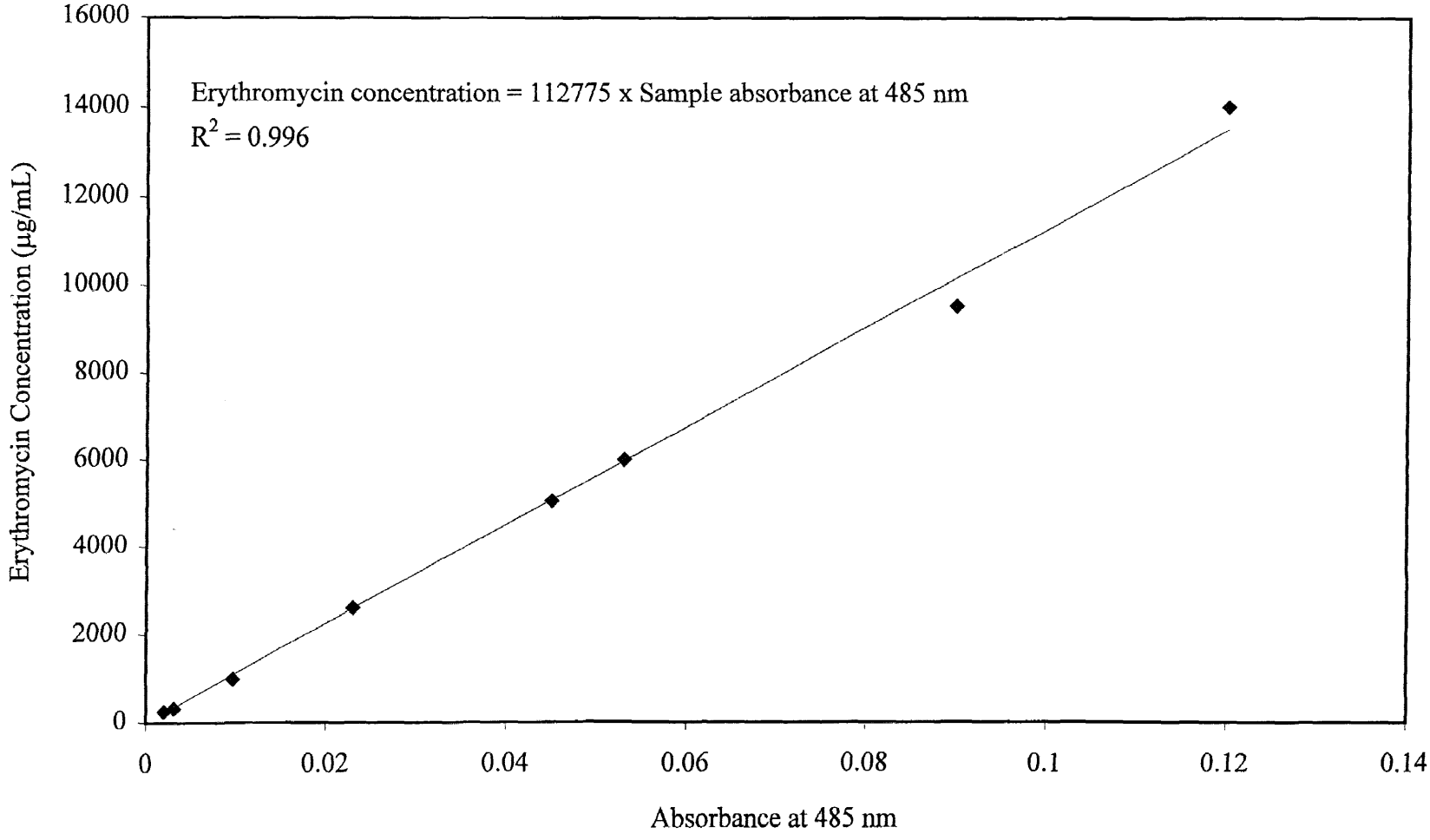

Figure 3.5 Calibration Curve for the Analysis of Erythromycin Concentration

erythromycin concentration during nanofiltration and diafiltration experiments. Calibration curves were prepared from fresh, standard dilute solutions of erythromycin in methanol to relate the concentration of a solution with the absorbance measured at λ_{max} (485 nm).

3.6.2 Analysis for Ethyl Acetate

Ethyl acetate concentration in methanol was measured in a gas chromatograph (model HP 6890) using a headspace sampler (model HP 7694). The output of the gas chromatograph was connected to an integrator (model HP 6890). The sample was analyzed by a flame ionization detector using a 30 m long, 320 μm diameter and 1 μm film thickness HP-5 capillary column containing crosslinked 5 % PH ME Siloxane (Hewlett Packard, Wilmington, DE). Ultrapure nitrogen was used as the carrier gas.

The technique employed for analysis was based on complete transfer of analytes from the liquid phase into the vapor phase. This eliminated the possibility of contamination of the analytes from any nonvolatile component in the sample, namely erythromycin. Reproducible results were obtained by delivering 3 μL of sample in a 22.5 mL headspace vial. The headspace oven temperature was maintained at 70°C with a sample equilibration time of 7 minutes. The vapors generated in the headspace were analyzed in the gas chromatograph according to a fixed temperature program in which the initial oven temperature of 40°C was maintained for 1.5 minutes and then raised to 80°C at the rate of 3°C/minute. The carrier gas flow was maintained at 50 mL/minute. Figure 3.6 shows the calibration curve for the gas chromatograph analysis.

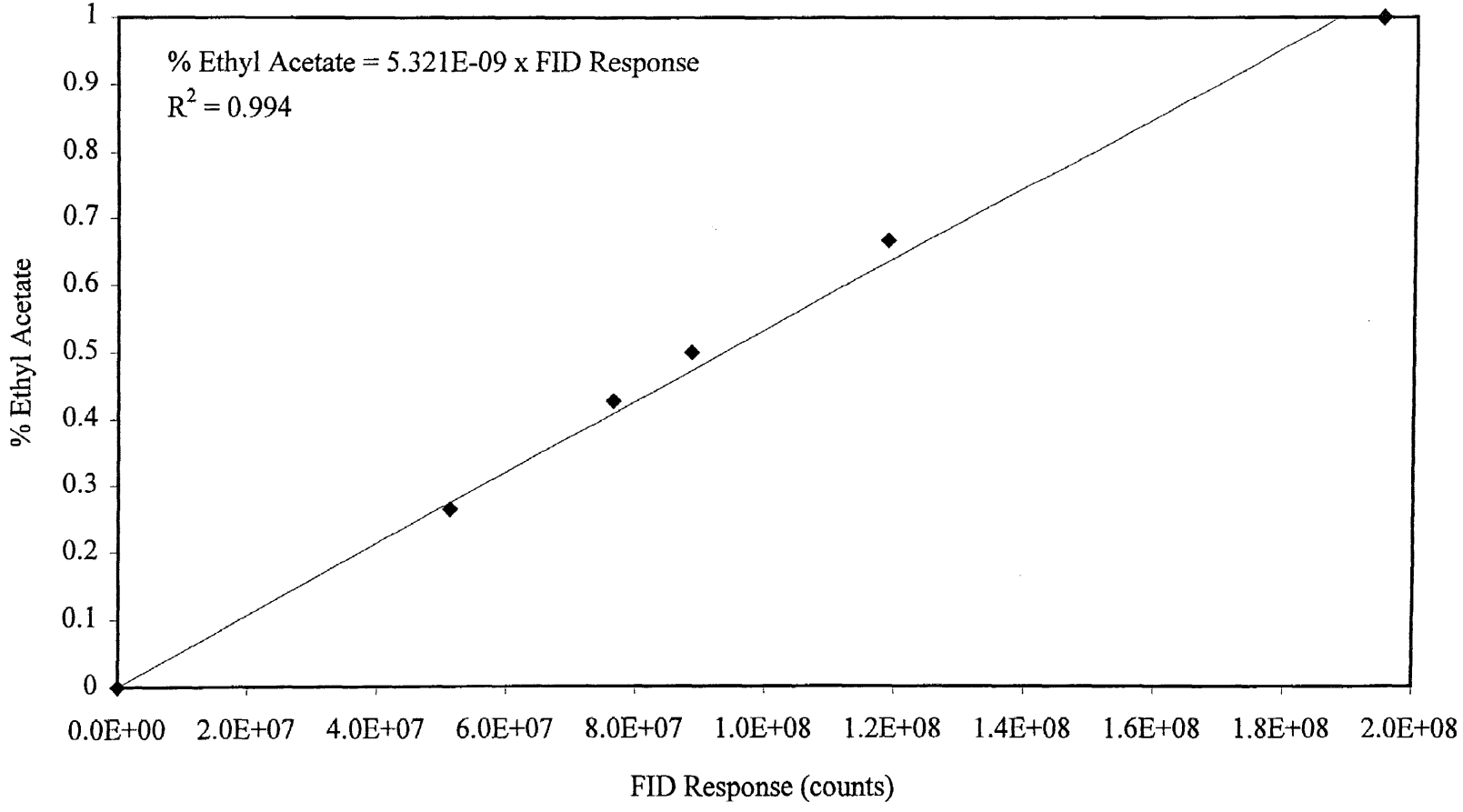

Figure 3.6 Calibration Curve for the Analysis of Ethyl Acetate Concentration in Permeate

CHAPTER 4

RESULTS AND DISCUSSION

Time-dependent results for nanofiltration and diafiltration operations are presented and discussed in this chapter. Permeate flux profiles of pure solvents during nanofiltration operation are also presented. The time-dependent behavior of the membrane is studied from two perspectives, permeate flux profile and solute rejection profile. The effect of mixed solvent environment on membrane performance during diafiltration operation is also presented and discussed. Sample calculations for permeate flux and solute rejection are provided in Appendix B.

4.1 Membrane Behavior and Permeate Flux Profile in Pure Solvent Environment

MPF-50 and MPF-60 membrane samples were tested several times at 440 psig (3033.8 kPa) and room temperature under stirred cell conditions. Methanol and ethyl acetate permeate flux profiles for MPF-50 and MPF-60 membranes are shown in Figures 4.1 and 4.2 as a function of the operation time.

It is seen that the nature of the permeate flux profiles for both solvents, methanol and ethyl acetate, follow a similar trend through the nanofiltration membranes. The results show that the permeate flux was highest during the initial period of each test run. A gradual declining trend in the permeate flux profile was observed thereafter. Moreover, the permeate flux was the highest during the initial period of the test run for a fresh membrane sample. Both MPF-50 and MPF-60 are flat sheet microporous anisotropic polymeric membranes supported on porous supports. In general, under a sustained

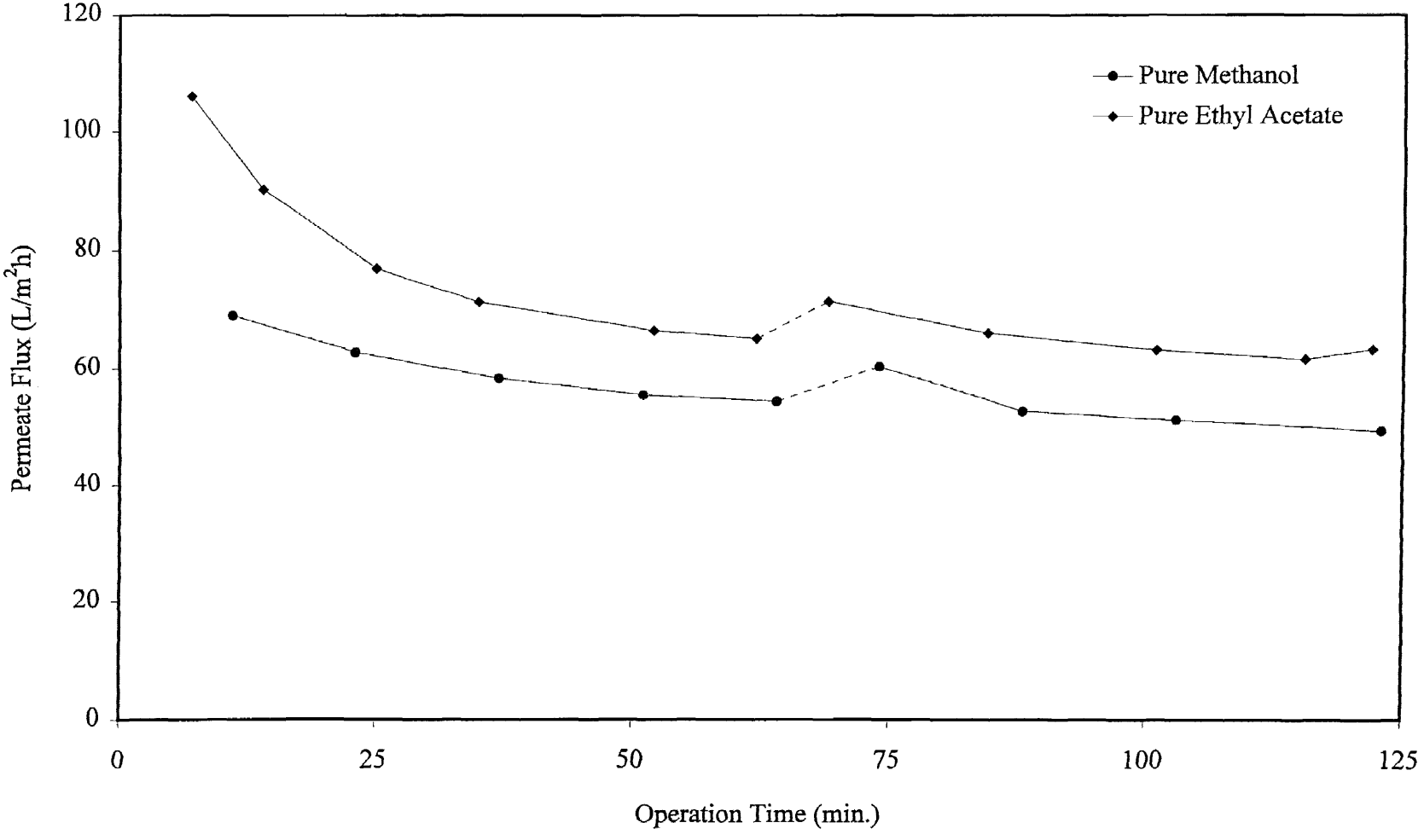

Figure 4.1 Permeate Flux as a Function of Operation Time for MPF-50 Membrane (Operation Conditions: Starting Feed=Pure Solvent, 440 psig, room temperature, stirred cell)

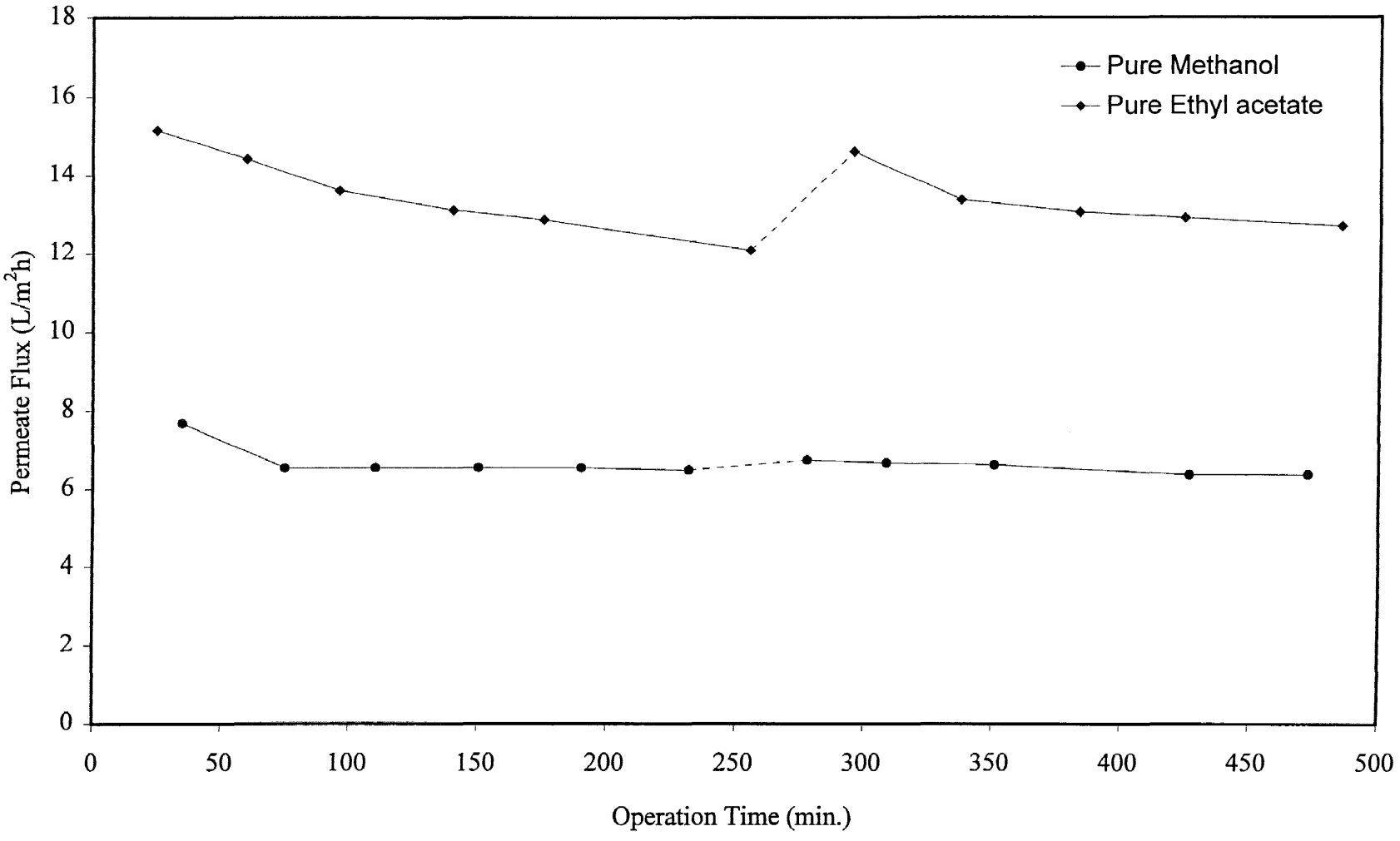

Figure 4.2 Permeate Flux as a Function of Operation Time for MPF-60 Membrane (Operation Conditions: Starting Feed=Pure Solvent, 440 psig, room temperature, stirred cell)

pressure load, such membranes gradually undergo compaction. Membrane porosity and pore size decrease as a result of this compaction. Due to the reduction in membrane pore size, the permeate flux through such membranes declines over the operation time (Eisold, et al., 1990). As can be seen from Figures 4.1 and 4.2, both MPF-50 and MPF-60 membranes exhibit a similar trend in their permeate flux profile, irrespective of the solvent environment. During actual applications involving solutes, both in aqueous or organic solutions, it is difficult to distinguish between the effect of membrane compaction and membrane fouling on such a declining permeate flux profile. However, in the present case due to the absence of any solutes, membrane compaction was primarily responsible. Preconditioned and fresh MPF-50 and MPF-60 membrane samples were used to test each solvent and subsequent tests were performed on the same membrane. However, as can be seen from Figures 4.1 and 4.2, the permeate flux during the initial period of each test run was higher than that at the end of the previous test. This suggests that membrane compaction, whose onset was seen during the first test, was partially reversible.

Table 4.1 Summary of Nanofiltration Experiments with Pure Solvents

Membrane	Solvent	Test Conditions		Permeate Flux (L/m^2h)			
		Pressure (psig)	Temp	First Run		Second Run	
				Initial	Final	Initial	Final
MPF-50	Methanol	440	Room	68.89	54.05	60.00	49.34
	Ethyl acetate	440	Room	106.02	64.74	71.05	63.16
MPF-60	Methanol	440	Room	7.67	6.45	6.70	6.35
	Ethyl acetate	440	Room	15.16	12.04	14.61	12.68

Table 4.1 provides a summary of initial and final values of the permeate flux for each test run. The membrane, however, did not completely recover its original properties, since the permeate flux during the initial period of the test run was lower for each subsequent test. Another consequence of membrane compaction is the decrease in membrane thickness. Permeate flux is inversely proportional to membrane thickness (eq. 2.1). Hence, the decrease in membrane thickness should lead to a higher permeate flux. But the effect of a smaller pore size and porosity seems to offset any increase in flux due to a decrease in membrane thickness

4.1.1 Solvent Properties and Permeate Flux

The permeate fluxes of ethyl acetate through MPF-50 and MPF-60 membranes were consistently higher than those of methanol. Such a result can be attributed to the differences in several properties of the two solvents. Table 4.2 gives a summary of some important solvent properties relevant in the present context.

In general it has been found that the permeate flux through a polymeric nanofiltration membrane depends upon the solvent structure properties such as molecular

Table 4.2 Pure Solvent Properties (CRC Handbook, 1998 and Van der Bruggen et al., 1998)

Solvent	Molecular Weight (daltons)	Polarity	Viscosity at 25 °C (m.Pa.s)	Surface Tension at 25 °C (N.m/m)	Dielectric Constant at 20 °C	Stokes Dia. (nm)	Equiv. Molar Dia. (nm)
MeOH	32.04	High	0.544	22.07	33.0	0.51	0.51
EtAC	88.11	Moderate	0.423	23.39	6.0814	0.86	0.68

size, molecular weight, solvent molecule polarity, and charge on solvent molecule. Furthermore, some solvent properties such as viscosity, surface tension, dipole moment, and Hildebrand solubility parameter are important parameters in determining the permeate flux through the membrane. Higher polarity of the solvent decreases the permeate flux, whereas lower viscosity and surface tension facilitate higher flux through the membrane. The effects of the molecular size and dielectric constant on solvent flux were observed to be relatively small (Machado et al., 1999).

In the case of methanol and ethyl acetate, as can be seen from the Table 4.2, the viscosity of ethyl acetate is lower than that of methanol by approximately 28 % at 25 °C. At the same time methanol is more polar than ethyl acetate. The combined effects of these two parameters lead to a lower methanol permeate flux as compared to that of ethyl acetate. This can be seen from Figures 4.1 and 4.2. Surface tension of methanol is only slightly lower (approximately 6 % at 25 °C) than that of ethyl acetate. Hence, even though lower surface tension of a solvent leads to a higher permeate flux through the membrane, in the case of methanol and ethyl acetate, the much higher viscosity of methanol (combined with its higher polarity) offsets the favorable effect of surface tension on permeate flux. Thus in the present case, the viscosity and polarity of the two solvents seem to be the dominant properties in determining the relative magnitude of the solvent permeate flux through the membrane. The molecular weight and molecular size of methanol are much smaller than that of ethyl acetate. However, the low molecular weight cut off (MWCO) of the MPF membranes (as compared to the two solvents) suggests that the membrane-solvent interaction properties are more important than solvent structure properties in determining permeate flux through the membrane.

4.2 Nanofiltration of a Given Solution

Membranes MPF-50 and MPF-60 were used to carry out nanofiltration experiments using solutions of erythromycin in ethyl acetate. The experiments were carried out at 440 psig (3033.8 kPa) and room temperature. Table 4.3 provides a summary of the experiments performed. Permeate flux as a function of operation time follows a declining trend similar to that of the pure solvent (discussed in previous section). Rejection on the other hand exhibits a steadily increasing trend. Nanofiltration runs were carried out long enough for the membrane rejection to reach a steady state. Figures 4.3 and 4.4 illustrate the permeate flux and rejection profiles of MPF 50 and MPF-60 membranes, respectively.

Table 4.3 Summary of Nanofiltration Experiments with Ethyl Acetate Solutions.

Membrane	Solute	Starting Feed Conc. (μg/mL)	Stirring	Test Conditions	
				Pressure (psig)	Temperature
MPF-50	Erythromycin	5000	Yes	440	Room
MPF-60	Erythromycin	5000	Yes	440	Room

4.2.1 Permeate Flux Profile

In the case of pure solvents, the declining permeate flux can be attributed to the gradual compaction of the polymeric nanofiltration over the operation time. A similar trend observed in case of solutions can be explained by three other factors in addition to membrane compaction. These are apparent membrane permeability, solute osmotic pressure and membrane pore crowding by and membrane adsorption of solute molecules. Equation (2.1) states that the permeate flux is directly dependent upon the apparent

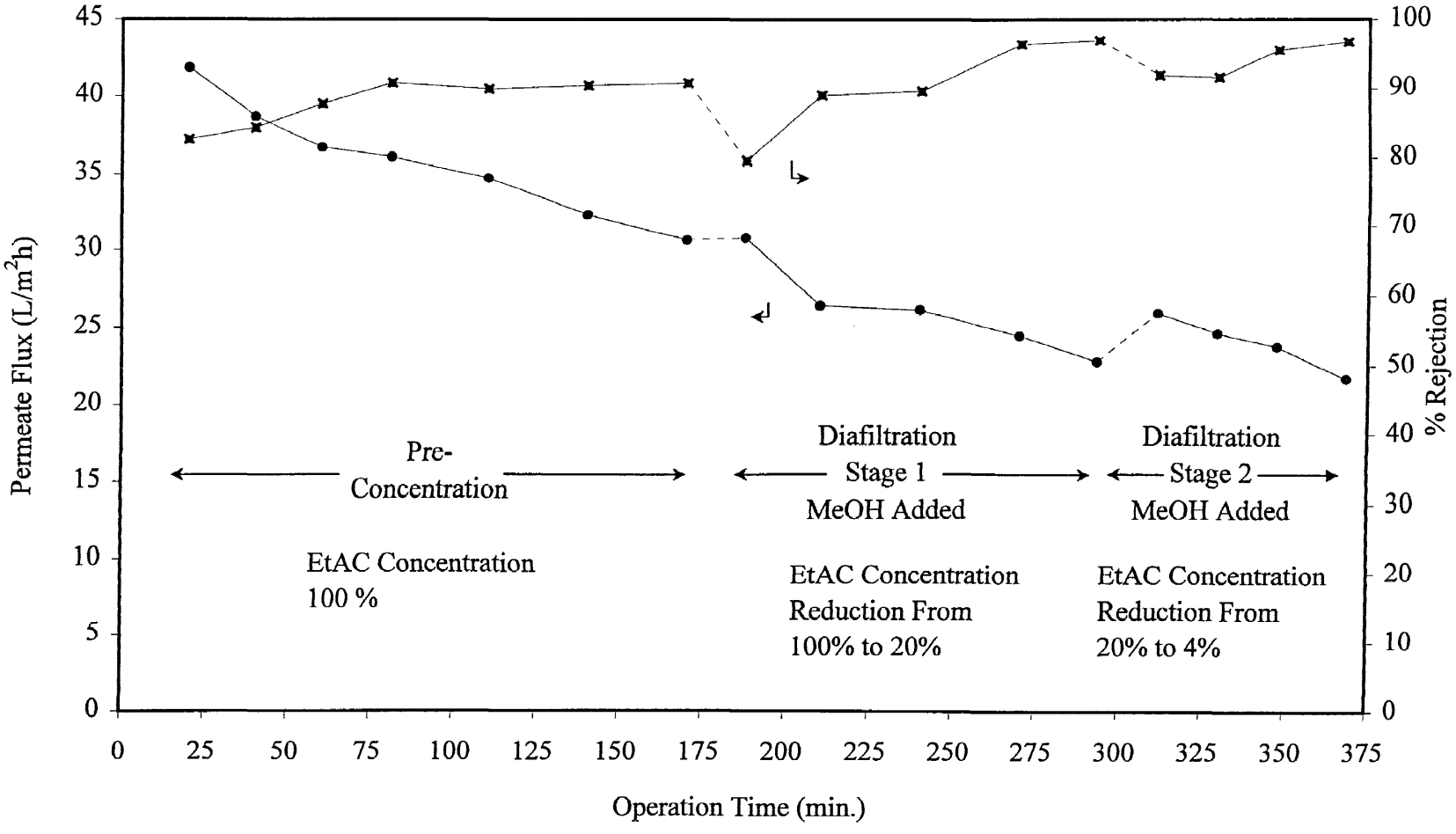

Figure 4.3 Permeate Flux and Solute Rejection as a Function of Operation Time for MPF-50 Membrane (Operation Conditions: Starting Feed = 5000 μg/mL Erythromycin in EtAC, 440 psig, room temperature, stirred cell)

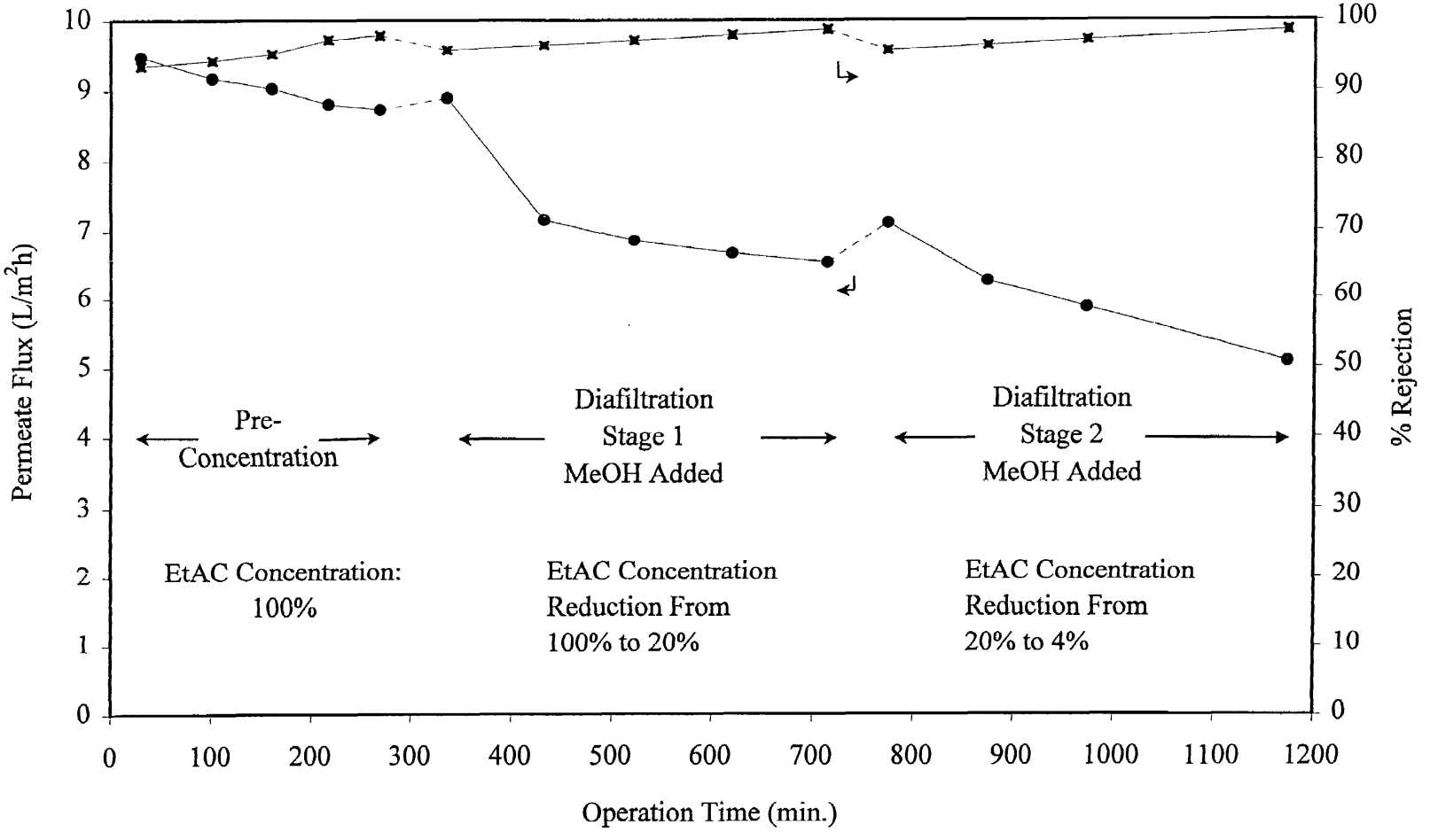

Figur 4.4 Permeate Flux and Solute Rejection as a Function of Operation Time for MPF-60 Membrane (Operation Conditions: Starting Feed = 5000 μg/mL Erythromycin in EtAC, 440 psig, room temperature, stirred cell)

membrane permeability and the net pressure difference across the membrane. The osmotic pressure of dilute solutions (concentration less than 0.2M) can be estimated by the Van't Hoff law for osmotic pressure (Atkins 1994; Nabetani et al, 1992) which is given below,

$$\pi = M_i RT \tag{4.1}$$

Over the entire nanofiltration run for all the experiments performed, the concentration of the solution inside the membrane cell (retentate) never exceeded 22000 μg/mL or approximately 0.03M erythromycin in ethyl acetate. At this concentration the osmotic pressure generated was less than 11 psi (assuming a very dilute permeate). Considering the applied pressure difference across the membrane of 440 psig (3033.8 kPa), the osmotic pressure constitutes only a 2.5 % reduction in this pressure. Hence it can be concluded that the effect of osmotic pressure on permeate flux was negligible. Furthermore, the presence of solute molecules in the solvent gives rise to frictional forces that oppose permeate flux. These frictional forces reduce the apparent permeability of the membrane. However, the frictional forces generated cannot be very high because of the dilute concentration of the solution. Hence, membrane compaction, osmotic pressure or apparent membrane permeability cannot explain an order of magnitude decrease (as seen from table 4.4) in the permeate flux through the membrane.

Such a significant decrease in permeate flux can be explained by the crowding effect of the retentate on the active side of the membrane. Although the membrane pore dimensions are not available, it is postulated that due to the relatively small difference in the molecular weight of erythromycin (MW 734) and the molecular weight cut-off of MPF-50 (MWCO 700) and MPF-60 (MWCO 400) membrane, the molecular dimensions

of erythromycin are of the same order of magnitude as the average pore size of the membranes. Furthermore, the membrane pore size distribution leads to a presence of some pores whose dimensions are larger than the average pore size. Hence it was possible that some solute molecules entered the membrane pores and blocked them partially or in some cases even completely. This significantly increased the membrane resistance to permeate flux. Additionally there is a significant possibility of solute adsorption in the pores which will also reduce the permeate flux. At the end of a nanofiltration run, formation of a gel layer was not observed in any of the experiments performed. Hence the drastic reduction in permeate flux through the membrane can be attributed to the membrane pore blockage / adsorption by solute molecules and not to any concentration polarization effects.

Table 4.4 Comparison of Initial Permeate Fluxes of Pure Solvents and Solutions

Membrane	Solution	Permeate Flux * (L/m^2h)
MPF-50	Pure ethyl acetate	76.8
	5000 μg/mL erythromycin in ethyl acetate	41.04
MPF-60	Pure ethyl acetate	15.16
	5000 μg/mL erythromycin in ethyl acetate	9.47

* Flux after 25 minutes of operation.

4.2.2 Solute Rejection Profile

Rejection profiles of both MPF-50 and MPF-60 membranes followed a steadily increasing trend with operation time. Table 4.5 provides a summary of initial and steady

state rejection values of both membranes. As can be seen from Table 4.5, the MWCO of MPF-50 is 700, but the erythromycin (MW 734) rejection never reaches the 95 % value used to specify the MWCO of a membrane. In case of MPF-60, even though the molecular weight of erythromycin is well above the MWCO of the membrane, it is unable to completely reject the solute. Hence it can be concluded that the specified MWCO of a membrane is an inadequate indication of the rejection characteristics of the membrane. MWCO has been traditionally used to indicate the rejection characteristics of a given membrane. However, this study and research conducted by others (Whu et al., 2000; Van der Bruggen et al., 1999) have found the need for an appropriate model describing the rejection profile of a membrane as a function of molecular size parameters, to replace MWCO as the sole indicator of membrane rejection behavior.

Table 4.5 Summary of Erythromycin Rejection by MPF-50 and MPF-60 Membranes

Membrane	MWCO	Solute	% Rejection	
			Initial	Steady State
MPF-50	700	Erythromycin	82.7	92.8
MPF-60	400	Erythromycin	93.4	97.9

Note: Starting Feed Concentration = 5000 μg/mL

Operation conditions: 440 psig (3033.8 kPa), room temperature, stirred cell.

4.3 Diafiltration of Nanofiltered Solutions

In multi step organic synthesis, consecutive reactions are often carried out in different solvent media. The solvent medium used in one reaction step often acts as an impurity for the next reaction step and hence must be reduced below a certain concentration. Such a

situation was simulated by replacing ethyl acetate with methanol. As explained above, the solution of erythromycin in ethyl acetate was concentrated by nanofiltration. The retentate thus obtained was subjected to diafiltration with methanol. In two consecutive diafiltration steps, the ethyl acetate concentration in the retentate was reduced to less than approximately 20 % and 4% by volume, respectively. Dilution with methanol can further bring down the concentration of ethyl acetate in the retentate to the required concentration level.

Table 4.6 Summary of Erythromycin Rejection by MPF-50 and MPF-60 Membranes

Membrane	MWCO	Solute	% Rejection			
			Diafiltration 1		Diafiltration 1	
			Initial	Steady State	Initial	Steady State
MPF-50	700	Erythromycin	79.6	97.0	91.9	96.8
MPF-60	400	Erythromycin	95.8	98.8	95.6	98.6

Note: Operation conditions: 440 psig (3033.8 kPa), room temperature, stirred cell.

Diafiltration experiments were carried out by using MPF-50 and MPF-60 membranes that had been already compacted by a nanofiltration run. The experiments were conducted at 440 psig (3033.8 kPa) and room temperature. Two consecutive solvent exchange runs were carried out for each membrane sample. A starting solution of erythromycin in ethyl acetate was first pre-concentrated by nanofiltration and then diluted by pure methanol, for the first diafiltration run, so that the concentration of ethyl acetate in the diluted solution was approximately 20 %. For the second diafiltration run, pure

methanol was again added to the retentate such that the concentration of ethyl acetate in this solution was approximately equal to 4%. Figures 4.3 and 4.4 show the permeate flux and solute rejection profiles during diafiltration. Figures 4.5 and 4.6 describe the concentration of ethyl acetate in the permeate during the course of the diafiltration runs. Table 4.6 contains a brief summary of the rejection values of MPF-50 and MPF-60 membranes.

4.3.1 Permeate Flux Profile in Mixed Solvent Environment

The permeate flux of erythromycin in ethyl acetate and methanol mixture through the MPF-50 and MPF-60 membranes followed a trend similar to that of pure solvents or solution of erythromycin in ethyl acetate alone. In general, the fluxes were lower than those observed for the previous nanofiltration experiment. This was because of two reasons. First, the feed solution was approximately 80 % methanol for the first diafiltration run and approximately 96 % for the second diafiltration run. For reasons mentioned above, the flux of methanol through the nanofiltration membranes is inherently lower than that of ethyl acetate. Also, as can be seen from Figures 4.5 and 4.6, both MPF-50 and MPF-60 exhibited no selectivity for either ethyl acetate or methanol. Hence, as can be seen from Figures 4.3 and 4.4, the permeate flux was systematically lower for each consecutive diafiltration run. Secondly, since the membranes had been already used for the pre-concentration (by nanofiltration) runs, some of their pores had already been blocked by the adsorbed solute (erythromycin) molecules. This led to a considerably higher membrane resistance to permeate flux.

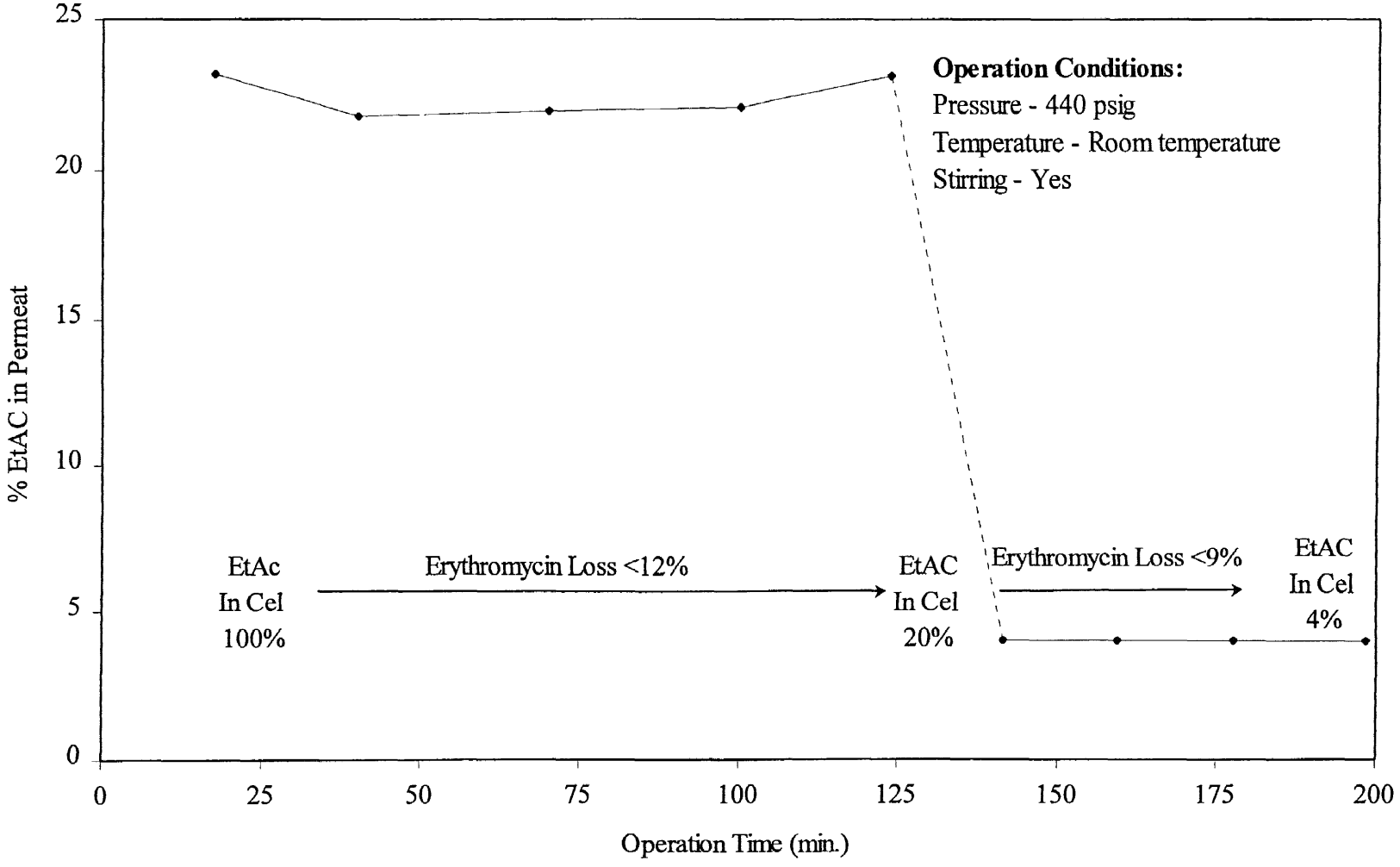

Figure 4.5 Permeate Concentration as a Function of Operation Time, During Solvent Exchange for MPF-50 Membrane: Diafiltration Operations

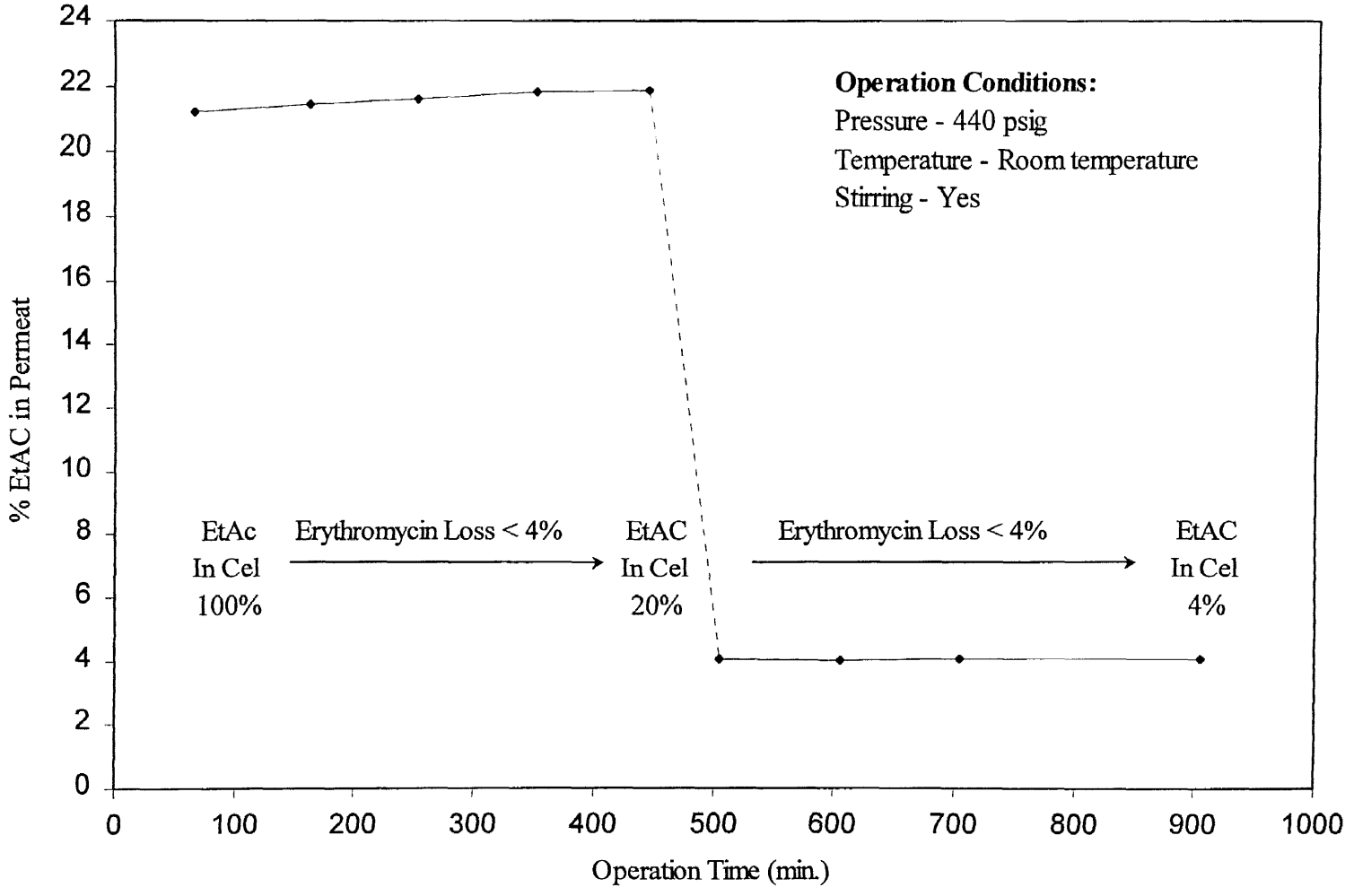

Figure 4.6 Permeate Concentration as a Function of Operation Time, During Solvent Exchange for MPF-60 Membrane : Diafiltration Operations

The lack of selectivity exhibited by both MPF-50 and MPF-60 membranes to methanol and ethyl acetate mixtures can be explained by the very large difference between the molecular weights of methanol (MW 32.04) and ethyl acetate (MW 88.11) and molecular weight cut-offs of MPF-50 (MWCO 700) and MPF-60 (MWCO 400).

4.3.2 Erythromycin Rejection Profile During Diafiltration

The rejection of erythromycin in ethyl acetate and methanol mixture through the MPF-50 and MPF-60 membranes followed a trend similar to that exhibited during the pre-concentration (nanofiltration) of erythromycin in ethyl acetate solution. Table 4.7 gives the percent loss of erythromycin during each experiment.

Table 4.7 Erythromycin Loss during Nanofiltration and Diafiltration Experiments

Membrane	% Erythromycin Loss During an Entire Experiment		
	Nanofiltration	Diafiltration 1	Diafiltration 2
MPF-50	16.1	11.14	8.74
MPF-60	3.63	3.64	3.63

As can be seen from Table 4.7, the erythromycin loss steadily decreased with each successive run for MPF-50 membrane. This was despite the fact that the starting feed concentrations in diafiltration runs 1 and 2 were more dilute, approximately 4200 μg/mL and 3750 μg/mL respectively, as compared to 5000 μg/mL for the nanofiltration run. In the case of MPF-60, the starting feed concentration for the two diafiltration runs was only half as that for the nanofiltration run. In previous studies (Whu et al., 2000) it was found that solute rejection is directly proportional to feed concentration. Therefore, the steady

increase in erythromycin rejection over the entire length of the experiment for both MPF-50 and MPF-60 membranes is indicative of the progressive membrane fouling by the solute, erythromycin. Appendix C contains an erythromycin mass balance for the entire nanofiltration-diafiltration runs performed with MPF-60 membrane.

CHAPTER 5

CONCLUSIONS AND RECOMMENDATIONS FOR FUTURE WORK

5.1 Conclusions

Nanofiltration as a separation technique has traditionally been used to separate dissolved ionic species from wastewaters. More recently, due to the cost effectiveness of nanofiltration over reverse osmosis, nanofiltration is finding increasing favor in the field of liquid separations. However, most of the research efforts, both in industry and academia, have been dedicated to aqueous solutions. In the present work, an effort has been made to study nanofiltration of organic systems, as applicable to the pharmaceutical industry in particular and the chemical process industry in general. The feasibility of nanofiltration in the field of organic synthesis was studied from two different operational stand points. In the first step an organic solution (erythromycin in ethyl acetate) was concentrated via nanofiltration and in the second step the solvent medium (ethyl acetate) was replaced by another solvent (methanol) via diafiltration stages. The following conclusions can be drawn from this study:

1. Polymeric nanofiltration membranes undergo considerable compaction under a sustained pressure load. Hence their performance is time dependent. This affects the permeance and rejection characteristics of the membrane. It was found that the solute rejection reached a steady state much earlier than permeate flux.
2. Solute loss decreased (as rejection increased) with each successive nanofiltration run. This gives an important insight into the membrane conditioning requirements and the mode of operation in large scale industrial applications. Solutes of interest, especially in the pharmaceutical industry, are expensive and hence the initial stages of the first

3. nanofiltration run (pre concentration) could be operated in a complete recycle mode, where the permeate (with a relatively high concentration of the expensive solute) is recycled until the membrane achieves a consistent high rejection of the solute. Also, in order to minimize the length of the initial unsteady behavior of the membranes, they could be pre compacted by exposure to pure solvents at operational pressure and temperature.
4. It was found that the nanofiltration membranes studied (MPF-50 and MPF-60) showed no selectivity when exposed to a mixed solvent feed. This underscored the importance of the pre-concentration stage, which the reduced the total amount of solution volume that had to be handled. By reducing the amount of the initial solution volume, a reduced volume of the second solvent was required to replace the first solvent within required levels. This technique has obvious economic implications for large scale industrial operations, where the permeate must be further processed (e.g. distillation) to separate the solvent mixture.
5. The manufacturer-specified MWCO was found to be an insufficient parameter for accurate prediction since the observed rejection values were slightly lower than that predicted by MWCO.
6. One potential advantage of this separation technique from the pollution prevention perspective was realized through this study. Most chemical reactions in the pharmaceutical industry produce a low molecular weight by-product that must be separated from the intermediate product of interest by a separation technique that involves a solvent (e.g. extraction). However, the present nanofiltration technique can simultaneously remove the solvent and the low molecular weight by-product, since

the MWCO of the nanofiltration membranes is generally much lower as compared to these by-products. Hence nanofiltration can reduce the total amount of solvents required, facilitate separation by using fewer different solvents and minimize the number of post processing operations required.

5.2 Recommendations for Future Work

Through the present study, the feasibility of nanofiltration as a separation technique in organic synthesis of pharmaceutical products was realized. A better understanding of some other aspects, stated below, can further facilitate the potential use of this technique in the pharmaceutical industry.

1. A need for a model, based on molecular dimensions, to indicate the rejection capability of commercially available solvent stable membrane can be developed. This would make the membrane selection procedure for an application more reliable.
2. In the present work every effort was made to study an industrially relevant system. Further investigative efforts can be made on a "real-world" multi-step reaction system, consisting of an intermediate (solute of interest) and its by-product. This system could be also studied for long-term performance.
3. Solvent exchange via diafiltration was performed in a discontinuous mode. A continuous operation mode can facilitate better control of the operation and eliminate the need for the various pressurization cycles.

APPENDIX A

MOLECULAR STRUCTURE OF ERYTHROMYCIN

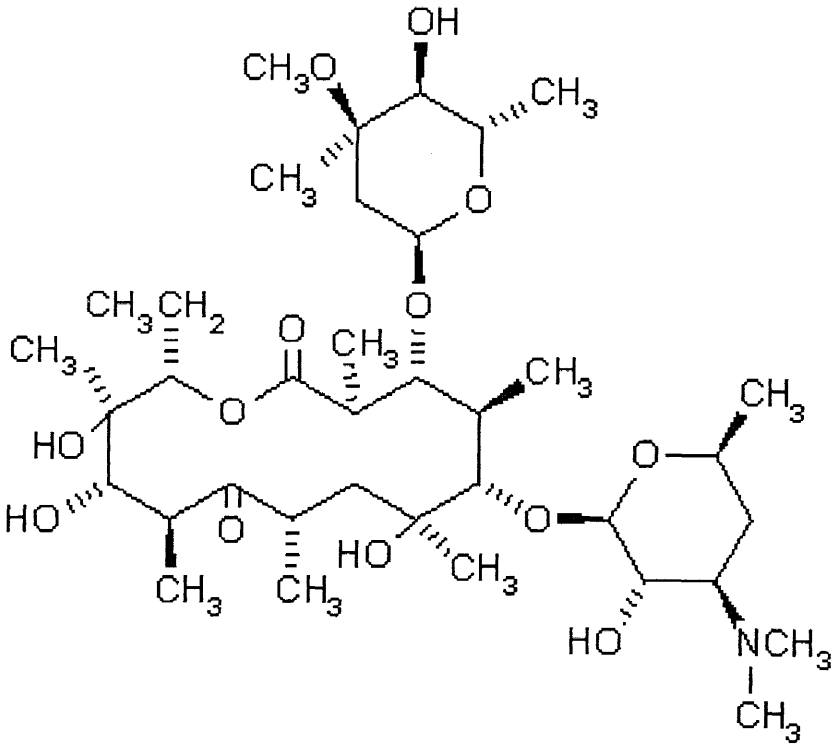

Figure A Molecular Structure of Erythromycin

APPENDIX B

SAMPLE CALCULATIONS FOR AVERAGE PERMEATE FLUX AND SOLUTE REJECTION

Average permeate flux and solute rejection results for MPF-60 membrane, shown in Chapter 4, are tabulated in Tables B.1 and B.2 respectively. Formulae used to calculate the flux and rejection values are also presented in addition to a sample calculation for permeate sample 2. Operation conditions are shown below each table.

The average permeate flux (shown in Table B.1) is given by,

$$Avg.\ permeate\ flux\ \left(\frac{L}{m^2 h}\right)\Big|_i = \frac{Permeate\ volume\ collected\ (mL)\,|_i \times 600}{Sample\ time\ (min)\,|_i \times Effect.\ membrane\ area\ (cm^2)} \quad (A.1)$$

Hence, for permeate sample 2, we have,

$$Avg.\ permeate\ flux\ \left(\frac{L}{m^2 h}\right)\Big|_i = \frac{7.2\,(mL)\,|_i \times 600}{30\,(min)\,|_i \times 15.2\,(cm^2)} = 9.47\left(\frac{L}{m^2 h}\right)$$

The % rejection was calculated on the basis of the average solute concentration in the permeate and the retentate. A solute mass balance at the end of each sample provide the information required. Equations (A.2) to (A.5) illustrate the calculation procedure. Each equation is followed by a sample calculation for permeate sample 2.

$$Ret.vol.|_i = Ret.vol.|_{i-1} - Perm.vol.|_i \quad (A.2)$$

$$Ret.vol.(mL)|_i = 100\,(mL)|_{i-1} - 7.2\,(mL)|_i = 92.8\,(mL)$$

$$Sol.conc.in\ ret.|_i = \frac{\left(Sol\ conc.in\ ret.|_{i-1}\ X\ ret.vol.|_{i-1}\right) - \left(Sol.conc.in\ perm.|_i\ X\ perm.vol.|_i\right)}{\mathrm{Re}t.vol.|_i} \tag{A.3}$$

$$Sol.conc.in\ ret.\left(\frac{\mu g}{mL}\right)\Big|_i = \frac{\left[5000\left(\frac{\mu g}{mL}\right)\Big|_{i-1} X\,100\,(mL)|_{i-1}\right] - \left[\left[341\left(\frac{\mu g}{mL}\right)\Big|_i X\,7.2\,(mL)|_i\right]\right]}{92.8\,(mL)|_i}$$

$$= 5361.47\left(\frac{\mu g}{mL}\right)$$

$$Avg.sol.conc.in\ ret.|_i = \frac{Sol.conc.in\ ret.|_{i-1} + sol.conc.in\ ret|_i}{2} \tag{A.4}$$

$$Avg.sol.conc.in\ ret.\left(\frac{\mu g}{mL}\right)\Big|_i = \frac{5000\left(\frac{\mu g}{mL}\right)\Big|_{i-1} + 5361.47\left(\frac{\mu g}{mL}\right)\Big|_i}{2} = 5180.74\left(\frac{\mu g}{mL}\right)$$

$$\%\ Rejection = \left(1 - \frac{Sol.conc.in\ perm.|_i}{Avg.sol.conc.in\ ret.|_i}\right) x100 \tag{A.5}$$

$$\%\ Rejection = \left(1 - \frac{341\left(\frac{\mu g}{mL}\right)\Big|_i}{5180.74\left(\frac{\mu g}{mL}\right)\Big|_i}\right) x100 = 93.42\,\%$$

Table B.1 Sample Calculation of Average Permeate Flux Through MPF-60 Membrane

Sample	Sample Time (min.)	Cumulative Time (min.)	Permeate Collected (mL)	Average Flux (L/m^2h)
Pre-concentration				
1	30	30	7.2	9.47
2	71	101	16.5	9.17
3	59	160	13.5	9.03
4	56	216	12.5	8.81
5	52	268	11.5	8.73
Diafiltration 1				
6	67	335	15.1	8.90
7	96	431	17.4	7.15
8	90	521	15.6	6.84
9	98	619	16.5	6.65
10	94	713	15.5	6.51
Diafiltration 2				
11	60	773	10.8	7.11
12	100	873	15.8	6.24
13	100	973	14.8	5.84
14	200	1173	25.7	5.07

Operation conditions:

Effective membrane area: 15.2 cm^2

Starting feed: 5000 μg/mL erythromycin in ethyl acetate

Operation pressure: 440 psig (3033.8 kPa)

Temperature: Room

Stirring: Yes

Table B.2 Sample Calculation of Average Rejection of Erythromycin by MPF-60 Membrane

Sample	Permeate Collected (mL)	Solute Concetration in Permeate (μg/mL)	Retentate Volume (mL)	Solute Concetration in Retentate (μg/mL)	Avg. Solute Concetration in Retentate (μg/mL)	% Rejection
Pre-concentration						
Feed ⟶			100.00	5000.00		
1	7.20	341.00	92.80	5361.47	5180.74	93.42
2	16.50	341.00	76.30	6447.16	5904.32	94.22
3	13.50	341.00	62.80	7759.79	7103.47	95.20
4	12.50	227.30	50.30	9631.68	8695.74	97.39
5	11.50	227.30	38.80	12419.06	11025.37	97.94
Diafiltration 1						
Feed ⟶			100.00	2500.00		
6	15.10	113.64	84.90	2924.43	2712.21	95.81
7	17.40	113.64	67.50	3648.99	3286.71	96.54
8	15.60	113.64	51.90	4711.64	4180.31	97.28
9	16.50	113.64	35.40	6854.77	5783.20	98.03
10	15.50	113.64	19.90	12105.40	9480.08	98.80
Diafiltration 2						
Feed ⟶			84.00	2500.00		
11	10.80	113.64	73.20	2852.09	2676.04	95.75
12	15.80	113.64	57.40	3605.87	3228.98	96.48
13	14.80	113.64	42.60	4819.14	4212.51	97.30
14	25.70	113.64	16.90	11974.84	8396.99	98.65

Operation conditions:

Effective membrane area: 15.2 cm^2

Starting feed: 5000 μg/mL erythromycin in ethyl acetate

Operation pressure: 440 psig (3033.8 kPa)

Temperature: Room

Stirring: Yes

APPENDIX C

MASS BALANCE DURING PRE-CONCENTRATION AND DIAFILTRATION STEPS FOR MPF-60 MEMBRANE

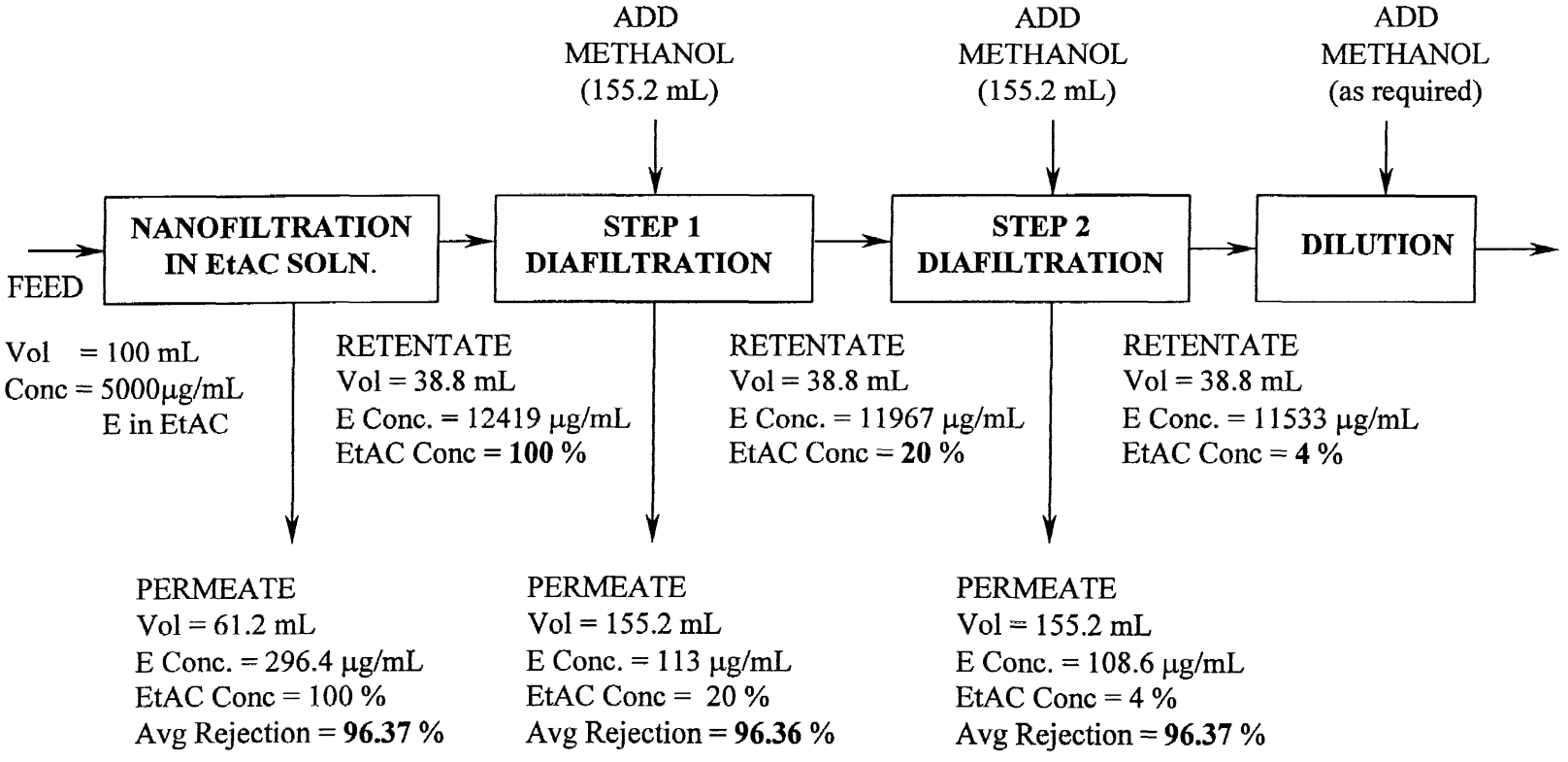

REFERENCES

Amy, G. L. "Removal of Dissolved Organic Matter by Nanofiltration," *J. Environmental Engr.*, 116, p.200 (**1990**).

Ary, S., "Ultrapure Water Application," *International Conference on Membranes, Chicago*, IL (**1990**).

Asbi, B. A., and M. Cheryan, "Optimizing Process Time for Ultrafiltration and Diafiltration," *Desalination*, 86, p.49 (**1992**).

Bindoff, A., C. J. Davies, C. A. Karr, and C. A. Buckley, "The Nanofiltration and Reuse of Effluent from the Caustic Extraction Stage of Wood Pulping ," *Ibid.*, 67, p.455 (**1987**).

Blatt, W. F., A. Dravid, A. S. Michaels, and L. Nelsen, "Solute Polarization and Cake Formation in Membrane Ultrafiltration: Causes, Consequences and Control Techniques," Membrane Science and Technology, ed. J. E. Flynn, Plenum Press, NY, (**1970**).

Bowen W. R., and A. W. Mohammad, "Diafiltration by Nanofiltration: Prediction and Optimization," *AIChE J.*, 44, 8 (**1998**).

Chen, L., and Z. Zhang, "Spectrophotometric Determination of the Content of Erythromycin," *Lihua Jianyan, Huaxue Fence*, CAN 120:62432, Journal written in Chinese (**1993**).

Chung, J., "Solvent Exchange in Bulk Pharmaceutical Manufacturing," *Pharmaceutical Technology*, June p.39 (**1996**).

CRC Handbook of Chemistry and Physics, 79th edition, CRC Press, NY (**1998**).

Culler, P. L., and S. A. McClellan, "A New Approach to Partial Demineralization," *50th Technical Conference of FS/AWWA-FPCA & FWPOCA*, Tampa, FL (**1976**).

Dutre, B., and G. Tragardh, "Macrosolute-Microsolute Separation by Ultrafiltration: A Review of Diafiltration Processes and Applications," *Desalination*, 95, p.227 (**1994**).

Eisold, C., H. H. Schwarz, and H. Buschatz, "Methods for Determination of Membrane Compaction," *Inst. Polymerenchem*, 42, 1, CAN 112:161087, Journal written in German (**1990**).

REFERENCES
(Continued)

Eriksson P., "Nanofiltration Extends the Range of Membrane Filtration," *AIChE Annual Meeting*, Miami Beach, Florida (**1986**).

Hagmeyer, G., and R. Gimbel, "Modeling the Rejection of Nanofiltration Membranes Using Zeta Potential Measurements," *Sep. and Purif. Tech.*, 15, p.19 (**1999**).

Ho Winston, W. S., and K. K. Sirkar, (ed.), Membrane Handbook, Chapman and Hall, NY (**1992**).

Jaffrin, M. Y., and J. Ph. Charrier, "Optimization of Ultrafiltration and Diafiltration Processes for Albumin Production," *J. Membr Sci.*, 97, p.71 (**1994**).

KOCH Membrane Systems: Fluid Systems, "SelRO®Nanofiltration Membranes and Modules," *Technical Data Sheets*: MPF-50 and MPF-60 Membranes (**1999**).

Lonsdale R., U. Merten, and R. L. Riley, "Transport Properties of Cellulose Acetate Osmonic Membranes," *J. Appl. Poly. Sci.*, 9 1341 (**1965**).

Machdo D. R., D. Hasson, and R. Semiat, "Effect of Solvent Properties on Permeate Flow Through Nanofiltration Membranes. Part I: Investigation of Parameters Affecting Solvent Flux," *J. Membr. Sci.*, 163, p.93 (**1999**).

Machdo, D. R., D. Hasson, R. Semiat, "Effect of Solvent Properties on Permeate Flow Through Nanofiltration Membranes. Part II: Transport Model," *Ibid.*, 163, p.63 (**1999**).

Macoun, R. G., Y. R. Shen, A. G. Fane, and C. J. D. Fell, "Nanofiltration: Theory and Applications to Ionic Separations", *Chemeca 91*, Newcastle, Australia (**1991**).

Merten, U., Desalination by Reverse Osmosis, The M.I.T. Press, Cambridge, MA (**1966**).

Morrison, F. A., and J. F. Osterle, "Electrokinetic Energy Conversion in Ultrafine Capillaries," *J. Chem. Phys.*, 43, 6 (**1965**).

Nguyen, Q. T., P. Aptel, and J. Neel, " Characterization of Ultrafiltration Membranes: Part I," *J. Membr. Sci.*, 5 (**1979**).

Niwa, M., H. Ohya, E. Kuwuhara, Y. Negishi, "Reverse Osmosis Concentration of Aqueous 2-Butanone (Methyl Ethyl Ketone), Tetrahydrofuran and Ethyl Acetate Solutions," *J. Chem. Eng. Jpn*, 21 (**1988**).

REFERENCES
(Continued)

Oikawa, E., K. Katoh, T. Aoki, "Characteristics of Reverse Osmosis Membranes Prepared From Schiff Bases of Polyallylamine of Aprotic Solvents and Separation of Organic and Inorganic Solutes Through the Membranes ," *Sep. Sci. Tech.*, 26 (**1991**).

Paul, D. H., "Back to Basics: Understanding Nanofiltration Membranes," *Ultrapure Water*, 15, 6 (**1998**).

Paul, E. L., and C. B. Rosas, "Challenges for Chemical Engineers in the Pharmaceutical Industry," *Chem Eng. Prog.*, 86, 17 (**1990**).

Pontalier, P. Y., A. Ismail, and M. Ghoul, "Mechanisms for Selective Rejection of Solutes in Nanofiltration Membranes," *Sep. Sci. and Tech.*, 12 (**1997**).

Porter, M. C., Handbook of Industrial Membrane Technology, ed. M. C. Porter, Noyes Publications, NJ (**1988**).

Puri, P. S., "Membrane Gas Separations: An Opportunity for Gas Industry or Just A Niche Market," *ICOM 99*, Toronto (**1999**).

Raman P. L., M. Cheryan, and N. Rajagoplan, "Consider Nanofiltration for Membrane Separations," *Chem. Eng. Prog.*, 90 p.68 (**1994**).

Reddy, K. K., T. Kawakatsu, J. B. Snape, and M. Nakajima, "Membrane Concentration and Separation of L-Aspartic Acid and L-Phenylalnine Derivatives in Organic Solvents," *Sep. Sci. Tech.*, 31 (**1996**).

Rogers R., "Membrane Materials Market to Grow Steadily," *Chem. & Eng. News*, 76, 34 (**1998**).

Rosa, M. J., and M. N. Pinho, "Separation of Organic Solutes by Membrane Pressure Driven Processes," *J. Membr. Sci.*, 89 p.173 (**1994**).

Shanley, A., "Membranes Push the Envelope," *Chemical Engineering*, 106, 5 (**1999**).

Tsuru, T., T. Shutou, S. I. Nakao and S. Kimura, "Peptide and Amino Acid Separation with Nanofiltration Membranes," *Sep. Sci. and Tech.*, 29, 8 (**1994**).

Uragami, T., M. Tamura, and M. Sugihara, "Synthesis and Permeability of Special Polymer Membranes. XII. Ultrafiltration and Adsorption Characteristics of Cellulose Acetate Nitrate-Activated Charcoal Membranes," *J. Membr. Sci.*, 4 (**1979**).

REFERENCES
(Continued)

Van der Bruggen, B., J. Schaep, D. Wilms, and C. Vandecasteele, "Influence of Molecular Size, Polarity and Charge on the Retention of Organic Molecules by Nanofiltration," *Ibid.*, 156, p.29 (**1999**).

Wang, X. L., T. Tsuru, M. Togoh, S.I. Nakao, and S. Kimura, "Evaluation of Pore Structure and Electrical Properties of Nanofiltration Membranes," *J. Chem. Eng. Jpn*, 28, 2 (**1995**).

Wang, X. L., T. Tsuru, S. I. Nakao, and S. Kimura, "Electrolyte Transport Through Nanofiltration Membranes by the Space-Charge Model and the Comparison with Torell-Meyer-Sievers Model," J. *Membr. Sci.*, 103, p.117 (**1995**).

Wang, X. L., T. Tsuru, S.I. Nakao, and S. Kimura, "The Electrostatic and Streic Hindrance Model for the Transport of Charged Solutes through Nanofiltration Membranes," *Ibid.*, 135, p.19 (**1997**).

Watson, D., and C. D. Hornburg, "Low Energy Membrane Nanofiltraion for Removal of Color Organics and Hardness fromn Water Supplies," *Desalination*, 72 p.11 (**1989**).

Whu, J., B. C. Baltzis and K. K. Sirkar, "Modeling of Nanofiltration-Assisted Organic Synthesis," *J. Membr. Sci.*, 163, p.163 (**1999**).

Whu, J., B. C. Baltzis and K. K. Sirkar, "Nanofiltration Studies of Large Organic Microsolutes in Methanol Solutions," *Ibid.*, 170, p.159 (**2000**).